Using Probability Density Functions to Derive Consistent Closure Relationships among Higher-Order Moments

VINCENT E. LARSON

Atmospheric Science Group, Department of Mathematical Sciences, University of Wisconsin—Milwaukee, Milwaukee, Wisconsin

JEAN-CHRISTOPHE GOLAZ

National Research Council, Naval Research Laboratory, Monterey, California

(Manuscript received 29 December 2003, in final form 29 July 2004)

ABSTRACT

Parameterizations of turbulence often predict several lower-order moments and make closure assumptions for higher-order moments. In principle, the low- and high-order moments share the same probability density function (PDF). One closure assumption, then, is the shape of this family of PDFs. When the higher-order moments involve both velocity and thermodynamic scalars, often the PDF shape has been assumed to be a double or triple delta function. This is equivalent to assuming a mass-flux model with no subplume variability. However, PDF families other than delta functions can be assumed. This is because the assumed PDF methodology is fairly general.

This paper proposes closures for several third- and fourth-order moments. To derive the closures, the moments are assumed to be consistent with a particular PDF family, namely, a mixture of two trivariate Gaussians. (This PDF is also called a double Gaussian or binormal PDF by some authors.) Separately from the PDF assumption, the paper also proposes a simplified relationship between scalar and velocity skewnesses. This PDF family and skewness relationship are simple enough to yield simple, analytic closure formulas relating the moments. If certain conditions hold, this set of moments is specifically realizable. By this it is meant that the set of moments corresponds to a real Gaussian-mixture PDF, one that is normalized and nonnegative everywhere.

This paper compares the new closure formulas with both large eddy simulations (LESs) and closures based on double and triple delta PDFs. This paper does not implement the closures in a single-column model and test them interactively. Rather, the comparisons are diagnostic; that is, low-order moments are extracted from the LES and treated as givens that are input into the closures. This isolates errors in the closures from errors in a single-column model. The test cases are three atmospheric boundary layers: a trade wind cumulus layer, a stratocumulus layer, and a clear convective case. The new closures have shortcomings, but nevertheless are superior to the double or triple delta closures in most of the cases tested.

1. Introduction

There has long been interest in higher-order turbulence closure models of the clear and cloudy boundary layer in the earth's atmosphere. Such models often predict central moments of vertical velocity w and thermodynamic scalars such as total specific water content q_t (a conserved variable, namely, the sum of vapor and liquid water) and liquid water potential temperature θ_l (a conserved variable that reduces to potential temperature in the absence of liquid).

Higher-order turbulence models are subject to the so-called closure problem. For instance, a prognostic moment equation of given order inevitably contains a higher-order moment that represents the turbulent flux of that quantity. To cite a specific example, the prognostic equation for the grid-box-averaged variance of q_t, $\overline{q_t'^2}$, contains the vertical turbulent flux of $\overline{q_t'^2}$, $\overline{w'q_t'^2}$. The closure problem, then, is to solve for unclosed moments, such as $\overline{w'q_t'^2}$, in terms of prognosed moments, such as $\overline{q_t'^2}$. Sometimes closure is complicated by the fact that the prognosed and unclosed moments are numerous. Once the unclosed moments have been diagnosed, however, the lower-order moments can be prognosed for the next time step, and the whole process repeats, advancing the solution in time.

The present paper discusses a methodology to derive approximate, analytic closure formulas, namely, the assumed probability density function (PDF) method (Sommeria and Deardorff 1977; Mellor 1977; Smith 1990; Bony and Emanuel 2001; Larson et al. 2001;

Corresponding author address: Vincent E. Larson, Department of Mathematical Sciences, University of Wisconsin—Milwaukee, P.O. Box 413, Milwaukee, WI 53201.
E-mail: vlarson@uwm.edu

Tompkins 2002). The methodology is as follows. We assume a *family* of PDFs that is specified by a number of parameters. The family is chosen based on simplicity and agreement with data. This paper assumes that the family is the sum of two Gaussians. For each grid box and time step, the higher-order model prognoses a set of moments. From the point of view of the closure problem, these are taken as known quantities or givens. Then from the assumed family of PDFs, we select a particular member for each grid box and time step by requiring it to be consistent with the prognosed moments. Once the PDF is specified, we can calculate from it whatever unclosed higher-order moments are needed. Then the closure is complete. For higher moments involving both w and q_t or θ_l, a simple PDF family, namely, a sum of two Dirac delta functions, has been used by meteorologists (Randall et al. 1992; Abdella and McFarlane 1997; Zilitinkevich et al. 1999; Lappen and Randall 2001) and engineers (e.g., Chung 2002, 775–778). Meteorologists have also used a sum of three Dirac delta functions (Mironov et al. 1999; Abdella and Petersen 2000; Gryanik and Hartmann 2002). This paper explores a new PDF family designed to better represent the atmospheric boundary layer.

The assumed PDF method has several advantages. First, it allows one to derive a large number of moments in an internally consistent manner (e.g., Lappen and Randall 2001). In other words, if a valid joint PDF can be specified from the lower-order moments, then all higher-order moments derived from it are consistent with the same joint PDF. This is more attractive than using separate closure assumptions for all the many moments that typically must be closed. Second, the method offers physical insight into the closure relations: namely, because a PDF is used to derive the moment closure formulas, those formulas can be interpreted in terms of the shape of the PDF. Third, the method has some generality: if the closure formulas turn out not to be suitable for a particular physical problem, one can seek an alternative PDF family, which will lead to alternative moment closures. A key point of this paper is that the assumed PDF methodology is not restricted to delta function PDFs, even when we need a joint PDF of w, θ_l, and q_t.

We desire closure formulas for the higher-order moments than can be written simply and analytically in terms of the lower-order moments. Analytical formulas are useful in part because they alert us to values of moments that give undefined results, for example, values that lead to division by zero. Furthermore, analytical formulas ease numerical implementation. In particular, they facilitate the implicit discretization of the higher-order turbulent advection terms in the model's prognostic equations. The implicit discretization, in turn, allows the use of a longer time step, thereby reducing computational cost. To obtain analytic closure formulas, we must first derive an analytic map that takes us from the known lower-order moments to the parameters that determine the PDF. We must then be able to write tractable formulas that take us from the PDF parameters to the unclosed higher-order moments. This restricts the complexity of the assumed PDF. The problem is especially acute because we want a *three-dimensional* joint PDF of w, q_t, and θ_l, and we want to permit nonzero skewness.

Although our motivation is the general problem of deriving analytic closure formulas, this paper will be restricted mainly to deriving closure equations for the higher-order boundary layer model of Golaz et al. (2002a, b). This model prognoses all first- and second-order moments (means and covariances) of w, q_t, and θ_l, and additionally prognoses the third-order moment of w, $\overline{w'^3}$. For the purpose of this paper, these are regarded as givens. The model requires closure of the following turbulent advection terms: $\overline{w'q_t'^2}$, $\overline{w'\theta_l'^2}$, $\overline{w'^2q_t'}$, $\overline{w'^2\theta_l'}$, $\overline{w'q_t'\theta_l'}$, and $\overline{w'^4}$. These are our unknowns. The model of Golaz et al. (2002a) also contains buoyancy and dissipation terms that need to be closed, but we do not consider them here. We desire a PDF family that is simple but general enough to adequately represent cumulus, stratocumulus, and clear boundary layers. We choose a trivariate mixture of Gaussians. It is a generalized version of the Analytic Double Gaussian 1 of Larson et al. (2002). Below we list a set of fairly nonrestrictive conditions (such as that the variances are positive) under which the derived moments are realizable. By this we mean that the prognosed and diagnosed moments correspond to a real PDF, namely one that is normalized and nonnegative everywhere.

We will compare various PDF-derived closures with three large eddy simulations (LESs). The simulated cases are a trade wind cumulus layer, a stratocumulus boundary layer, and a clear convective boundary layer. We compare the mixture of Gaussians PDF with two other PDFs that have served as the basis of closures in the meteorological literature: a mixture of two delta functions (Randall et al. 1992; Abdella and McFarlane 1997; Zilitinkevich et al. 1999; Lappen and Randall 2001), and a mixture of three delta functions (Mironov et al. 1999; Abdella and Petersen 2000; Gryanik and Hartmann 2002). The latter two PDFs correspond to mass-flux schemes with no within-plume variability (Randall et al. 1992; de Roode et al. 2000; Lappen and Randall 2001; Gryanik and Hartmann 2002). For conciseness, we do not investigate closures that are not derived purely from PDFs but instead include a downgradient diffusion term (Zilitinkevich et al. 1999) or the quasi-normal approximation (Canuto et al. 2001).

The present paper differs from Larson et al. (2002) because they discuss the diagnosis of cloud properties such as cloud fraction and liquid water content; here we instead investigate higher-order moments of conserved quantities. A further difference is that the present paper derives explicit formulas for higher-order moments in terms of lower-order moments; Larson et al. (2002) and Golaz et al. (2002b) merely wrote down higher-

order moments in terms of PDF parameters and left their relationship to lower-order moments implicit.

Major notation is summarized in appendix A.

2. The proposed PDF: A mixture of trivariate Gaussians

We now introduce a family of PDFs and show how to analytically specify the defining PDF parameters from a prescribed set of moments. The PDF is a modification of the Analytic Double Gaussian 1 of Larson et al. (2002), with the parameters specified using improved diagnostic formulas.

a. Functional form of the mixture of trivariate Gaussians

Our proposed PDF is a simplified mixture of trivariate Gaussians. The simplifications make the PDF less general but mathematically more tractable. The PDF depends on three variables: w, q_t, and θ_l. The chief advantages of the PDF for our purposes are that it permits both positive and negative skewness, and that it leads to an analytic closure.

For notational convenience, we will use normalized variables. For the thermodynamic scalars, we use a standardized form, denoted by a tilde, ~:

$$\tilde{\theta}_l' \equiv \frac{\theta_l - \overline{\theta_l}}{\sqrt{\overline{\theta_l'^2}}}, \tag{1}$$

$$\tilde{q}_t' \equiv \frac{q_t - \overline{q_t}}{\sqrt{\overline{q_t'^2}}}. \tag{2}$$

Here $\overline{\theta_l}$, $\overline{q_t}$, $\overline{\theta_l'^2}$ and $\overline{q_t'^2}$ are the means and variances of θ_l and q_t for the full PDF (not an individual Gaussian). We normalize variables that contain $w' = w - \overline{w}$ in a way that simplifies subsequent notation. We denote such variables by a hat, ^:

$$\hat{w}' \equiv \frac{w - \overline{w}}{\sqrt{\overline{w'^2}}} \frac{1}{(1 - \tilde{\sigma}_w^2)^{1/2}}. \tag{3}$$

Here $\overline{w}$ and $\overline{w'^2}$ are the mean and variance of w over the full PDF, including both Gaussians. Also, $\tilde{\sigma}_w = \sigma_w / \sqrt{\overline{w'^2}}$, where σ_w denotes the standard deviations (widths) of each individual Gaussian, which are set equal. Equation (3) centers and normalizes w. Making $\hat{w}'$ depend on $\tilde{\sigma}_w^2$ simplifies the subsequent equations by removing $\tilde{\sigma}_w^2$ except in the factors $\overline{w'^2}(1 - \tilde{\sigma}_w^2)$ and $\tilde{\sigma}_w^2/(1 - \tilde{\sigma}_w^2)$.

Our PDF, $P_{\text{tmg}}(\hat{w}', \tilde{\theta}_l', \tilde{q}_t')$, is a trivariate mixture of two Gaussians, G_1 and G_2:

$$P_{\text{tmg}}(\hat{w}', \tilde{\theta}_l', \tilde{q}_t') = aG_1(\hat{w}', \tilde{\theta}_l', \tilde{q}_t') + (1 - a)G_2(\hat{w}', \tilde{\theta}_l', \tilde{q}_t'). \tag{4}$$

Here, $0 < a < 1$ is the (nondimensional) mixture fraction. To simplify the mathematics, we prohibit each Gaussian, or "plume,"[1] from having any within-plume correlation between w and q_t, or between w and θ_l. Velocity–scalar correlations still arise from correlations between the two plumes. We do permit subplume correlation between q_t and θ_l, in order to improve agreement with atmospheric PDFs (Larson et al. 2002). The functional form of the ith Gaussian, where $i = 1$ or 2, is

$$(1 - \tilde{\sigma}_w^2)^{1/2} \sqrt{\overline{w'^2}\,\overline{\theta_l'^2}\,\overline{q_t'^2}}\, G_i(\hat{w}', \tilde{\theta}_l', \tilde{q}_t') = \frac{1}{(2\pi)^{3/2}[\tilde{\sigma}_w/(1 - \tilde{\sigma}_w^2)]^{1/2} \tilde{\sigma}_{q_t i} \tilde{\sigma}_{\theta_l i} (1 - r_{q_t\theta_l}^2)^{1/2}}$$
$$\times \exp\left\{ -\frac{1}{2}\left[\frac{\hat{w}' - \hat{w}_i}{\tilde{\sigma}_w/(1 - \tilde{\sigma}_w^2)^{1/2}} \right]^2 \right\} \times \exp\left\{ -\frac{1}{2(1 - r_{q_t\theta_l}^2)} \left[\left(\frac{\tilde{q}_t' - \tilde{q}_{ti}}{\tilde{\sigma}_{q_t i}} \right)^2 \right.\right.$$
$$\left.\left. + \left(\frac{\tilde{\theta}_l' - \tilde{\theta}_{li}}{\tilde{\sigma}_{\theta_l i}} \right)^2 - 2r_{q_t\theta_l} \left(\frac{\tilde{q}_t' - \tilde{q}_{ti}}{\tilde{\sigma}_{q_t i}} \right) \left(\frac{\tilde{\theta}_l' - \tilde{\theta}_{li}}{\tilde{\sigma}_{\theta_l i}} \right) \right] \right\}. \tag{5}$$

Here,

$$\tilde{\theta}_{li} \equiv \frac{\theta_{li} - \overline{\theta_l}}{\sqrt{\overline{\theta_l'^2}}}, \tag{6}$$

$$\tilde{q}_{ti} \equiv \frac{q_{ti} - \overline{q_t}}{\sqrt{\overline{q_t'^2}}}, \tag{7}$$

and

$$\hat{w}_i \equiv \frac{w_i - \overline{w}}{\sqrt{\overline{w'^2}}} \frac{1}{(1 - \tilde{\sigma}_w^2)^{1/2}}, \tag{8}$$

where the mean of the ith Gaussian is $(w_i, \theta_{li}, q_{ti})$. The parameters $\tilde{\sigma}_w = \sigma_w/\sqrt{\overline{w'^2}}$, $\tilde{\sigma}_{\theta_l i} = \sigma_{\theta_l i}/\sqrt{\overline{\theta_l'^2}}$, and $\tilde{\sigma}_{q_t i} = \sigma_{q_t i}/\sqrt{\overline{q_t'^2}}$ are normalized versions of the standard deviations σ_w, $\sigma_{\theta_l i}$, and $\sigma_{q_t i}$ of the ith Gaussian (5). Finally, $r_{q_t\theta_l}$ is the within-plume correlation of q_t and θ_l, which is

[1] A "plume" is defined here to be a mixture component of the PDF. Since the Gaussians may overlap, the plumes are not necessarily distinct or separable. For instance, each plume may contain both updrafts and downdrafts.

set equal for plumes 1 and 2, and must lie in the range −1 to 1.

b. A list of given moments and PDF parameters

The boundary layer model of Golaz et al. (2002a, b) prognoses the following 10 moments for each grid box and time step: $\overline{w}$, $\overline{w'^2}$, $\overline{w'^3}$, $\overline{\theta_l}$, $\overline{w'\theta_l'}$, $\overline{q_t}$, $\overline{w'q_t'}$, $\overline{\theta_l'^2}$, $\overline{q_t'^2}$, and $\overline{q_t'\theta_l'}$. We use these moments to specify a particular PDF within the family defined by (4) and (5). That is, we use the moments to determine the values of the 13 PDF parameters a, $\hat{w}_1$, $\hat{w}_2$, $\tilde{\theta}_{l1}$, $\tilde{\theta}_{l2}$, $\tilde{q}_{t1}$, $\tilde{q}_{t2}$, $\tilde{\sigma}_w$, $\tilde{\sigma}_{\theta_l 1}$, $\tilde{\sigma}_{\theta_l 2}$, $\tilde{\sigma}_{q_t 1}$, $\tilde{\sigma}_{q_t 2}$, and $r_{q_t\theta_l}$. To solve for the 13 unknowns in terms of the 10 knowns, we clearly need to make diagnostic assumptions; these are embedded in Eqs. (20)–(28) below.

c. Writing given moments in terms of PDF parameters

In this subsection, we list equations for moments in terms of PDF parameters. These are obtained by integrating the PDF, multiplied by the appropriate central moment (written to the left of each equation), over all possible values of w, q_t, and θ_l. For instance, the mean of w is obtained by $\overline{w} = \int_{-\infty}^{\infty} w P_{\text{tmg}} dw\ d\theta_l\ dq_t$. The equations are then rewritten in terms of centered, normalized variables:

$$w: \quad 0 = a\hat{w}_1 + (1-a)\hat{w}_2, \tag{9}$$

$$w'^2: \quad \frac{1}{(1-\tilde{\sigma}_w^2)} = a\left(\hat{w}_1^2 + \frac{\tilde{\sigma}_w^2}{(1-\tilde{\sigma}_w^2)}\right) + (1-a)\left(\hat{w}_2^2 + \frac{\tilde{\sigma}_w^2}{(1-\tilde{\sigma}_w^2)}\right), \tag{10}$$

$$w'^3: \quad \widehat{\text{Sk}}_w \equiv \frac{1}{(1-\tilde{\sigma}_w^2)^{3/2}} \frac{\overline{w'^3}}{(\overline{w'^2})^{3/2}} = a\left(\hat{w}_1^3 + 3\hat{w}_1 \frac{\tilde{\sigma}_w^2}{(1-\tilde{\sigma}_w^2)}\right) + (1-a)\left(\hat{w}_2^3 + 3\hat{w}_2 \frac{\tilde{\sigma}_w^2}{(1-\tilde{\sigma}_w^2)}\right), \tag{11}$$

$$\theta_l: \quad 0 = a\tilde{\theta}_{l1} + (1-a)\tilde{\theta}_{l2}, \tag{12}$$

$$\theta_l'^2: \quad 1 = a(\tilde{\theta}_{l1}^2 + \tilde{\sigma}_{\theta_l 1}^2) + (1-a)(\tilde{\theta}_{l2}^2 + \tilde{\sigma}_{\theta_l 2}^2), \tag{13}$$

$$q_t: \quad 0 = a\tilde{q}_{t1} + (1-a)\tilde{q}_{t2}, \tag{14}$$

$$q_t'^2: \quad 1 = a(\tilde{q}_{t1}^2 + \tilde{\sigma}_{q_t 1}^2) + (1-a)(\tilde{q}_{t2}^2 + \tilde{\sigma}_{q_t 2}^2), \tag{15}$$

$$w'\theta_l': \quad \hat{c}_{w\theta_l} \equiv \frac{1}{(1-\tilde{\sigma}_w^2)^{1/2}} \frac{\overline{w'\theta_l'}}{\sqrt{\overline{w'^2}}\sqrt{\overline{\theta_l'^2}}} \equiv \frac{c_{w\theta_l}}{(1-\tilde{\sigma}_w^2)^{1/2}} = a\hat{w}_1\tilde{\theta}_{l1} + (1-a)\hat{w}_2\tilde{\theta}_{l2}, \tag{16}$$

$$w'q_t': \quad \hat{c}_{wq_t} \equiv \frac{1}{(1-\tilde{\sigma}_w^2)^{1/2}} \frac{\overline{w'q_t'}}{\sqrt{\overline{w'^2}}\sqrt{\overline{q_t'^2}}} \equiv \frac{c_{wq_t}}{(1-\tilde{\sigma}_w^2)^{1/2}} = a\hat{w}_1\tilde{q}_{t1} + (1-a)\hat{w}_2\tilde{q}_{t2}, \tag{17}$$

$$q_t'\theta_l': \quad c_{q_t\theta_l} \equiv \frac{\overline{q_t'\theta_l'}}{\sqrt{\overline{q_t'^2}}\sqrt{\overline{\theta_l'^2}}} = a(\tilde{q}_{t1}\tilde{\theta}_{l1} + r_{q_t\theta_l}\tilde{\sigma}_{q_t 1}\tilde{\sigma}_{\theta_l 1}) + (1-a)(\tilde{q}_{t2}\tilde{\theta}_{l2} + r_{q_t\theta_l}\tilde{\sigma}_{q_t 2}\tilde{\sigma}_{\theta_l 2}). \tag{18}$$

We also list a moment that is diagnosed rather than prognosed [see Eq. (33) below]:

$$\theta_l'^3: \quad \text{Sk}_{\theta_l} \equiv \frac{\overline{\theta_l'^3}}{(\overline{\theta_l'^2})^{3/2}} = a(\tilde{\theta}_{l1}^3 + 3\tilde{\theta}_{l1}\tilde{\sigma}_{\theta_l 1}^2) + (1-a)(\tilde{\theta}_{l2}^3 + 3\tilde{\theta}_{l2}\tilde{\sigma}_{\theta_l 2}^2). \tag{19}$$

These equations are not restricted to mixtures of two Gaussians; they can also apply to mixtures of two non-Gaussian distributions. However, the equations are not general forms for mixtures of two distributions, because they make use of simplifying assumptions, such as that there is zero within-plume correlation of w and θ_l, and w and q_t; that the within-plume correlations of q_t and θ_l are equal for plumes 1 and 2; and that the within-plume skewness is zero.

d. Finding PDF parameters in terms of moments

We now select a particular member of our Gaussian-mixture family by mapping the prognosed moments to the PDF parameters. In other words, we invert Eqs. (9)–(18) in order to find the set of PDF parameters that guarantees that the resulting PDF has moments that correspond to the prognosed ones. The inversion is nontrivial because the equations are nonlinear in the PDF parameters. However, the PDF (4)–(5) is simple enough to permit an analytic solution.

The solution procedure is as follows. First, we solve

for the PDF parameters a, $\hat{w}_1$, and $\hat{w}_2$ from the moment equations for $\overline{w}$ (9), $\overline{w'^2}$ (10), $\overline{w'^3}$ (11):

$$a = \frac{1}{2}\left[1 - \widehat{\mathrm{Sk}}_w\left(\frac{1}{4 + \widehat{\mathrm{Sk}}_w^2}\right)^{1/2}\right], \tag{20}$$

$$\hat{w}_1 \equiv \frac{w_1 - \overline{w}}{\sqrt{\overline{w'^2}}}\frac{1}{(1-\tilde{\sigma}_w^2)^{1/2}} = \left(\frac{1-a}{a}\right)^{1/2}, \tag{21}$$

$$\hat{w}_2 \equiv \frac{w_2 - \overline{w}}{\sqrt{\overline{w'^2}}}\frac{1}{(1-\tilde{\sigma}_w^2)^{1/2}} = -\left(\frac{a}{1-a}\right)^{1/2}. \tag{22}$$

We have chosen, arbitrarily but without loss of generality, to set $\hat{w}_1 > \hat{w}_2$. Equation (20) implies that $\widehat{\mathrm{Sk}}_w$ is determined solely by a:

$$\widehat{\mathrm{Sk}}_w = \frac{1-2a}{[a(1-a)]^{1/2}}. \tag{23}$$

The temperature means of the individual plumes, $\tilde{\theta}_{l1}$ and $\tilde{\theta}_{l2}$, can be obtained from the equations for $\overline{\theta_l}$ (12) and $\overline{w'\theta_l'}$ (16):

$$\tilde{\theta}_{l1} \equiv \frac{\theta_{l1} - \overline{\theta_l}}{\sqrt{\overline{\theta_l'^2}}} = -\frac{\hat{c}_{w\theta_l}}{\hat{w}_2}, \tag{24}$$

$$\tilde{\theta}_{l2} \equiv \frac{\theta_{l2} - \overline{\theta_l}}{\sqrt{\overline{\theta_l'^2}}} = -\frac{\hat{c}_{w\theta_l}}{\hat{w}_1}. \tag{25}$$

The widths of the plumes, $\tilde{\sigma}_{\theta_l 1}$ and $\tilde{\sigma}_{\theta_l 2}$, are determined by satisfying the moment equations for $\overline{\theta_l'^2}$ (13) and $\overline{\theta_l'^3}$ (19):

$$\tilde{\sigma}_{\theta_l 1}^2 \equiv \frac{\sigma_{\theta_l 1}^2}{\overline{\theta_l'^2}} = (1 - \hat{c}_{w\theta_l}^2) + \left(\frac{1-a}{a}\right)^{1/2}\frac{1}{3\hat{c}_{w\theta_l}}(\mathrm{Sk}_{\theta_l} - \hat{c}_{w\theta_l}^3\widehat{\mathrm{Sk}}_w), \tag{26}$$

$$\tilde{\sigma}_{\theta_l 2}^2 \equiv \frac{\sigma_{\theta_l 2}^2}{\overline{\theta_l'^2}} = (1 - \hat{c}_{w\theta_l}^2) - \left(\frac{a}{1-a}\right)^{1/2}\frac{1}{3\hat{c}_{w\theta_l}}(\mathrm{Sk}_{\theta_l} - \hat{c}_{w\theta_l}^3\widehat{\mathrm{Sk}}_w). \tag{27}$$

Here Sk_{θ_l} is the skewness of θ_l. It must be provided either by a prognostic equation or by a diagnostic equation such as (33) below. Equations for $\tilde{q}_{t1}$, $\tilde{q}_{t2}$, $\tilde{\sigma}_{q_t 1}^2$, and $\tilde{\sigma}_{q_t 2}^2$ are found by expressions identical to (24), (25), (26), and (27), except that θ_l is replaced everywhere by q_t. Finally, from the equation for $\overline{q_t'\theta_l'}$ (18), we find

$$r_{q_t\theta_l} = \frac{c_{q_t\theta_l} - \hat{c}_{wq_t}\hat{c}_{w\theta_l}}{a\tilde{\sigma}_{q_t 1}\tilde{\sigma}_{\theta_l 1} + (1-a)\tilde{\sigma}_{q_t 2}\tilde{\sigma}_{\theta_l 2}}. \tag{28}$$

Here $r_{q_t\theta_l}$ is the subplume correlation; $c_{q_t\theta_l}$ is the total correlation. Finally, the parameter $\tilde{\sigma}_w^2$ is given by Eq. (37) below.

Equations (20)–(27) have the same content as Eqs. (A16)–(A22) of Larson et al. (2002) for the Analytic Double Gaussian 1 PDF. However, rewriting them in the present form emphasizes the similarity with the double delta function PDF. In fact, Eqs. (20)–(25) hold for the double delta PDF if the hats are dropped.

e. *Higher-order moments in terms of PDF parameters*

Once the PDF parameters have been specified, all higher-order moments can be calculated by integration over the PDF. The needed formulas are:

$$\frac{1}{(1-\tilde{\sigma}_w^2)^2}\frac{\overline{w'^4}}{(\overline{w'^2})^2} = a\left[\hat{w}_1^4 + 6\hat{w}_1^2\frac{\tilde{\sigma}_w^2}{(1-\tilde{\sigma}_w^2)} + 3\frac{\tilde{\sigma}_w^4}{(1-\tilde{\sigma}_w^2)^2}\right] + (1-a)\left[\hat{w}_2^4 + 6\hat{w}_2^2\frac{\tilde{\sigma}_w^2}{(1-\tilde{\sigma}_w^2)} + 3\frac{\tilde{\sigma}_w^4}{(1-\tilde{\sigma}_w^2)^2}\right], \tag{29}$$

$$\frac{\overline{w'^2\theta_l'}}{(1-\tilde{\sigma}_w^2)\overline{w'^2}(\overline{\theta_l'^2})^{1/2}} = a\left[\hat{w}_1^2 + \frac{\tilde{\sigma}_w^2}{(1-\tilde{\sigma}_w^2)}\right]\tilde{\theta}_{l1} + (1-a)\left[\hat{w}_2^2 + \frac{\tilde{\sigma}_w^2}{(1-\tilde{\sigma}_w^2)}\right]\tilde{\theta}_{l2}, \tag{30}$$

$$\frac{\overline{w'\theta_l'^2}}{(1-\tilde{\sigma}_w^2)^{1/2}(\overline{w'^2})^{1/2}\overline{\theta_l'^2}} = a\hat{w}_1(\tilde{\theta}_{l1}^2 + \tilde{\sigma}_{\theta_l 1}^2) + (1-a)\hat{w}_2(\tilde{\theta}_{l2}^2 + \tilde{\sigma}_{\theta_l 2}^2), \tag{31}$$

$$\frac{\overline{w'q_t'\theta_l'}}{(1-\tilde{\sigma}_w^2)^{1/2}(\overline{w'^2})^{1/2}(\overline{q_t'^2})^{1/2}(\overline{\theta_l'^2})^{1/2}} = a\hat{w}_1(\tilde{q}_{t1}\tilde{\theta}_{l1} + r_{q_t\theta_l}\tilde{\sigma}_{q_t 1}\tilde{\sigma}_{\theta_l 1}) + (1-a)\hat{w}_2(\tilde{q}_{t2}\tilde{\theta}_{l2} + r_{q_t\theta_l}\tilde{\sigma}_{q_t 2}\tilde{\sigma}_{\theta_l 2}). \tag{32}$$

The equations for $\overline{w'^2 q_t'}$ and $\overline{w' q_t'^2}$ are analogous to (30) and (31).

3. An additional assumption: A diagnostic ansatz for the skewness of heat and moisture

We cannot close the system of equations until we specify the skewness of θ_l, Sk_{θ_l}, which appears in the equations for $\tilde{\sigma}_{\theta_l 1}$ (26) and $\tilde{\sigma}_{\theta_l 2}$ (27). Likewise, we need to specify Sk_{q_t}. We could prognose these scalar skewnesses, but this would involve additional computational expense, storage, and complexity. In some cases, the extra complexity may be worthwhile. However, here we instead propose the following diagnostic formula:

$$\mathrm{Sk}_{\theta_l} = \widehat{\mathrm{Sk}}_w \hat{c}_{w\theta_l} [\beta + (1 - \beta)\hat{c}^2_{w\theta_l}], \tag{33}$$

and a similar formula for Sk_{q_t}. The parameter β is dimensionless. Any value of β from 0 to 3 is consistent with realizability. This formula is an empirical assumption that is separate from the assumption of the Gaussian-mixture PDF. It simply fixes the scalar skewness using a diagnostic formula rather than a prognostic equation. The quantity $|\mathrm{Sk}_{\theta_l}|$ increases with increasing β. When $\beta = 0$, the formula reduces to that (61) for a double delta function PDF. When $\beta = 1$, Sk_{θ_l} depends linearly on the heat flux correlation, $\hat{c}_{w\theta_l}$.

Equation (33) is physically plausible but limited at the same time. The formula states that Sk_{θ_l} is proportional to Sk_w, the skewness of w. An increase in β leads to an increase in $|\mathrm{Sk}_{\theta_l}|$, which, in turn, leads to a PDF with a longer θ_l-tail. The quantities Sk_{θ_l} and Sk_w have the same sign when w and θ_l are positively correlated; Sk_{θ_l} and Sk_w have opposite sign when w and θ_l are negatively correlated. In our large eddy simulations, this is usually but not always true. The quantity Sk_{θ_l} vanishes when either Sk_w or $c_{w\theta_l}$ vanishes; clearly this need not be true in nature. The quantity $|\mathrm{Sk}_{\theta_l}|$ can be either smaller or larger than $|\mathrm{Sk}_w|$, depending on the values of $\tilde{\sigma}^2_w$,$c_{w\theta_l}$ and β. In contrast, $|\mathrm{Sk}_{\theta_l}| \le |\mathrm{Sk}_w|$ by a factor of $|c^3_{w\theta_l}|$ for the double delta function PDF of Randall et al. (1992) [see Eq. (61) below].

Larson et al. (2002) used the following alternative diagnoses for the skewnesses: $\mathrm{Sk}_{\theta_l} = 0$ and $\mathrm{Sk}_{q_t} = 1.2\mathrm{Sk}_w$. Equation (33) has the following advantages over the formulas of Larson et al. (2002):

1) Because Eq. (33) for Sk_{θ_l} is proportional to $\hat{c}_{w\theta_l}$, using it in the equations for $\tilde{\sigma}_{\theta_l 1,2}$ [(26)–(27)] prevents these equations from becoming infinite in magnitude when $\hat{c}_{w\theta_l} \to 0$.
2) Because of the way $\hat{c}_{w\theta_l}$ enters Eq. (33), it satisfies the requirements of parity or reflectional symmetry (Mironov et al. 1999). That is, if θ_l changes sign everywhere in the equation, both sides of the equation change sign. The equation has even symmetry with respect to w.

   In contrast, the formula $\mathrm{Sk}_{q_t} = 1.2\mathrm{Sk}_w$ of Larson et al. (2002) does not obey the correct symmetry properties: if q_t changes sign, the left-hand side changes sign, but the right-hand side does not; and if w changes sign, the right-hand side changes sign, but the left-hand side does not. The practical problem with the formula $\mathrm{Sk}_{q_t} = 1.2\mathrm{Sk}_w$, which has incorrect symmetry properties, is that it is likely to yield the wrong sign for Sk_{q_t} when $\hat{c}_{wq_t} < 0$. However, usually atmospheric boundary layers have $\hat{c}_{wq_t} > 0$.
3) The skewness formula (33) can be shown to yield a realizable set of moments, when used in conjunction with the Gaussian-mixture PDF. By "realizable," we mean that when (33) is used in specifying the moments, the resulting Gaussian-mixture PDF is normalized and nonnegative everywhere. An unrealizable PDF would result, for instance, if Eqs. (26) and (27) were to yield negative plume widths. An example of this problem for the Analytic Double Gaussian 1 is shown in Fig. 4 of Larson et al. (2002), where a negative plume width occurs and has been set to zero.

If we assume our ansatz (33) for Sk_{θ_l}, then the θ_l widths of plumes 1 (26) and 2 (27) reduce to

$$\tilde{\sigma}^2_{\theta_l 1} = \frac{(1 - \hat{c}^2_{w\theta_l})}{a}\left[\frac{1}{3}\beta + a\left(1 - \frac{2}{3}\beta\right)\right] \tag{34}$$

and

$$\tilde{\sigma}^2_{\theta_l 2} = \frac{(1 - \hat{c}^2_{w\theta_l})}{1 - a}\left\{1 - \left[\frac{1}{3}\beta + a\left(1 - \frac{2}{3}\beta\right)\right]\right\}. \tag{35}$$

Substituting (34), (35), and their q_t counterparts into the expression for $r_{q_t\theta_l}$ (28) yields the simplified form:

$$r_{q_t\theta_l} = \frac{c_{q_t\theta_l} - \hat{c}_{wq_t}\hat{c}_{w\theta_l}}{(1 - \hat{c}^2_{wq_t})^{1/2}(1 - \hat{c}^2_{w\theta_l})^{1/2}}. \tag{36}$$

Here $r_{q_t\theta_l}$ is the within-plume correlation of q_t and θ_l; $c_{q_t\theta_l}$ is the total correlation.

We have not yet specified the w width of the individual plumes, $\tilde{\sigma}_w$. Larson et al. (2002) chose $\tilde{\sigma}^2_w = 0.4$. Here, instead we make $\tilde{\sigma}^2_w$ dependent on the maximum of $c^2_{wq_t}$ and $c^2_{w\theta_l}$:

$$\tilde{\sigma}^2_w = \gamma[1 - \max(c^2_{w\theta_l}, c^2_{wq_t})]. \tag{37}$$

Here $0 \le \gamma < 1$ is a dimensionless constant. This formula helps ensure that when c_{wq_t} or $c_{w\theta_l}$ becomes large in magnitude, $0 \le \hat{c}^2_{w\theta_l}, \hat{c}^2_{wq_t} < 1$ and hence $\tilde{\sigma}^2_{q_t 1,2}$, $\tilde{\sigma}^2_{\theta_l 1,2}$, and $r_{q_t\theta_l}$ remain realistic.

4. Proposed closures for third- and fourth-order moments based on the mixture of trivariate Gaussians

This section lists formulas for four higher-order moments that are needed for closure in the parameterization of Golaz et al. (2002a): $\overline{w'^4}$, $\overline{w'^2\theta_l'}$, $\overline{w'\theta_l'^2}$, and $\overline{w' q_t' \theta_l'}$. These are obtained by substituting the expres-

sions for the PDF parameters (20)–(28) into the equations for the higher-order moments (29)–(32). Formulas for $\overline{w'^2 q_t'}$ and $\overline{w' q_t'^2}$, which are also needed, are identical to those for $\overline{w'^2\theta_l'}$ and $\overline{w'\theta_l'^2}$ except that q_t replaces θ_l everywhere.

For convenience of the reader, we will list each formula twice: once in nondimensional form in order to illustrate their similarity with the double delta PDF; and once in dimensional form in order to list the formula that is plotted in the figures below and in order to show how $\tilde{\sigma}_w^2$ influences the higher-order moments.

First, we list the equation for $\theta_l'^3$, which is obtained by dimensionalizing (33):

$$\overline{\theta_l'^3} = \frac{1}{(1-\tilde{\sigma}_w^2)^2}\frac{\overline{w'^3}}{(\overline{w'^2})^2}\overline{\theta_l'^2}\,\overline{w'\theta_l'}\left(\beta + (1-\beta)\times\frac{1}{1-\tilde{\sigma}_w^2}\frac{(\overline{w'\theta_l'})^2}{\overline{w'^2}\,\overline{\theta_l'^2}}\right). \tag{38}$$

The scalar third moments are not needed to close the prognostic equations of Golaz et al. (2002a), but they do influence cloud properties, since cumulus clouds often reside on the tail of the scalar PDF. For typical parameter values, $\overline{\theta_l'^3}$ becomes larger with increases in $\tilde{\sigma}_w^2 = \sigma_w^2/\overline{w'^2}$, the relative width of the plumes in w [see Eq. (38)]. That is, $\overline{\theta_l'^3}$ increases as the marginal w-PDF becomes broader shaped and less like a double delta PDF.

The quantity $\overline{w'^4}$ does not depend on the thermodynamic scalar moments; therefore, it does not depend on β. Substituting (21) and (22) into (29) and using (23), we find

$$\frac{\overline{w'^4}}{(1-\tilde{\sigma}_w^2)^2(\overline{w'^2})^2} = 3\frac{\tilde{\sigma}_w^4}{(1-\tilde{\sigma}_w^2)^2} + 6\frac{\tilde{\sigma}_w^2}{(1-\tilde{\sigma}_w^2)} + 1 + \widehat{\mathrm{Sk}}_w^2, \tag{39}$$

$$\overline{w'^4} = (\overline{w'^2})^2(3\tilde{\sigma}_w^4 + 6(1-\tilde{\sigma}_w^2)\tilde{\sigma}_w^2 + (1-\tilde{\sigma}_w^2)^2) + \frac{1}{(1-\tilde{\sigma}_w^2)}\frac{(\overline{w'^3})^2}{\overline{w'^2}}. \tag{40}$$

We see from (40) that $\overline{w'^4}$ increases as $\tilde{\sigma}_w^2$ increases. If we set $\tilde{\sigma}_w^2 = 0.4$, a value that fits our LES reasonably well, we find that $\overline{w'^4} \cong (2.28 + 1.67\mathrm{Sk}_w^2)(\overline{w'^2})^2$. This formula is similar to that of Gryanik and Hartmann [2002, their Eq. (27)], namely, $\overline{w'^4} = (3 + \mathrm{Sk}_w^2)(\overline{w'^2})^2$. The latter formula interpolates between a single-Gaussian behavior for zero skewness and a double delta function behavior for large skewness.

Similar to $\overline{w'^4}$, $\overline{w'^2\theta_l'}$ does not depend on β for our particular PDF family. Substituting (21)–(25) into (30), we find

$$\frac{\overline{w'^2\theta_l'}}{(1-\tilde{\sigma}_w^2)\overline{w'^2}(\overline{\theta_l'^2})^{1/2}} = \hat{c}_{w\theta_l}\widehat{\mathrm{Sk}}_w, \tag{41}$$

$$\overline{w'^2\theta_l'} = \frac{1}{(1-\tilde{\sigma}_w^2)}\frac{\overline{w'^3}}{\overline{w'^2}}\overline{w'\theta_l'}. \tag{42}$$

In (42), $1/(1-\tilde{\sigma}_w^2)$ appears as a simple prefactor. Because we have derived this prefactor from an assumption about the shape of the PDF, we can give physical meaning to it. Namely, it is a simple function of the width of the plumes in w, and as the within-plume w variability increases, so does $\overline{w'^2\theta_l'}$. This prefactor is set to 1 by Mironov et al. (1999) and 1.8 by Abdella and Petersen (2000). If we use our Gaussian-mixture PDF, we see that $1/(1-\tilde{\sigma}_w^2) = 1$ corresponds to $\tilde{\sigma}_w^2 = 0$ (i.e., a double delta function PDF) and that $1/(1-\tilde{\sigma}_w^2) = 1.8$ corresponds to a moderate width of $\tilde{\sigma}_w^2 \cong 0.44$. The latter is close to the values that best fit our LES of clear and cloudy boundary layers.

The quantity $\overline{w'\theta_l'^2}$ depends explicitly on Sk_{θ_l}. Substituting (21)–(27) into (31) yields

$$\frac{\overline{w'\theta_l'^2}}{(1-\tilde{\sigma}_w^2)^{1/2}(\overline{w'^2})^{1/2}\overline{\theta_l'^2}} = \frac{2}{3}\hat{c}_{w\theta_l}^2\widehat{\mathrm{Sk}}_w + \frac{1}{3}\frac{\mathrm{Sk}_{\theta_l}}{\hat{c}_{w\theta_l}}, \tag{43}$$

$$\overline{w'\theta_l'^2} = \frac{2}{3}\frac{1}{(1-\tilde{\sigma}_w^2)^2}\frac{\overline{w'^3}}{(\overline{w'^2})^2}(\overline{w'\theta_l'})^2 + \frac{1}{3}(1-\tilde{\sigma}_w^2)\frac{\overline{w'^2}\,\overline{\theta_l'^3}}{\overline{w'\theta_l'}}. \tag{44}$$

Since $\overline{w'\theta_l'}$ appears in the denominator, this formula becomes singular as $\overline{w'\theta_l'}$ approaches zero. For this reason, if one uses this formula with observed values of $\overline{\theta_l'^3}$ and $\overline{w'\theta_l'}$, the diagnosis of $\overline{w'\theta_l'^2}$ can be quite noisy. We can remove the singularity by substituting in our ansatz for Sk_{θ_l} (33), or equivalently, Eq. (38) for $\overline{\theta_l'^3}$, which has $\overline{\theta_l'^3} \propto \overline{w'\theta_l'}$. Then we find

$$\frac{\overline{w'\theta_l'^2}}{(1-\tilde{\sigma}_w^2)^{1/2}(\overline{w'^2})^{1/2}\overline{\theta_l'^2}} = \widehat{\mathrm{Sk}}_w\left[\frac{1}{3}\beta + \left(1-\frac{1}{3}\beta\right)\hat{c}_{w\theta_l}^2\right], \tag{45}$$

$$\overline{w'\theta_l'^2} = \frac{1}{(1-\tilde{\sigma}_w^2)}\frac{\overline{w'^3}}{\overline{w'^2}}\left[\frac{1}{3}\beta\overline{\theta_l'^2} + \frac{\left(1-\frac{1}{3}\beta\right)}{(1-\tilde{\sigma}_w^2)}\frac{(\overline{w'\theta_l'})^2}{\overline{w'^2}}\right]. \tag{46}$$

One may make the following comments on this formula. The quantity $\overline{w'\theta_l'^2}$ is the turbulent transport of $\overline{\theta_l'^2}$. Roughly speaking, $\overline{w'\theta_l'^2} > 0$ if there is more temperature variability, $\theta_l'^2$, in updrafts than downdrafts, and vice versa. In the approximation (45), the sign of $\overline{w'\theta_l'^2}$ is determined solely by the sign of $\widehat{\mathrm{Sk}}_w$. The link between the sign of $\widehat{\mathrm{Sk}}_w$ and the corresponding variability in the two drafts is illustrated graphically in Fig. 1,

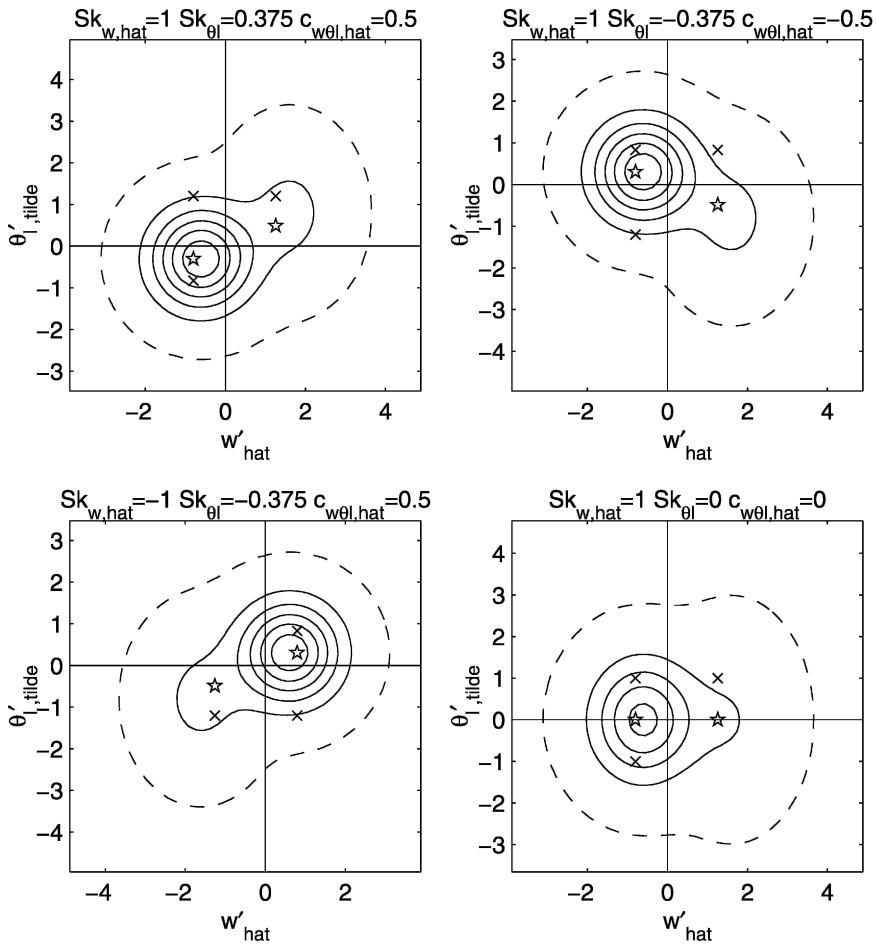

FIG. 1. Examples of three PDF families: the mixture of two trivariate Gaussian (contours), the double delta function (stars), and the triple delta function (x). The dashed contour is at 1% of the PDF maximum; the solid contours are evenly spaced. The subplots vary the values of scaled velocity skewness ($\widehat{\mathrm{Sk}}_w$), scalar skewness (Sk_{θ_l}), and scaled correlation ($\hat{c}_{w\theta_l}$). For all subplots, $\beta = 0.8$ and $\tilde{\sigma}_w^2 = 0.4$. The double delta function is chosen to match $\widehat{\mathrm{Sk}}_w$ and $\hat{c}_{w\theta_l}$, but it does not and cannot in general also match Sk_{θ_l}. The triple delta function is chosen to match $\widehat{\mathrm{Sk}}_w$ and Sk_{θ_l}, but it does not and cannot in general match $\hat{c}_{w\theta_l}$. Note that the double delta function tends to underpredict the scalar variance, $\overline{\theta_l'^2}$, especially in the lower-right panel. It also usually underpredicts Sk_{θ_l}. The triple delta function matches $\overline{\theta_l'^2}$ and Sk_{θ_l} exactly.

described below. In Eq. (45), $|\overline{w'\theta_l'^2}|$ is increased by an increase in β, as is $|\mathrm{Sk}_{\theta_l}|$.

Finally, substituting (21)–(28) into (32) yields the following formula for the turbulent flux of $\overline{q_t'\theta_l'}$, $\overline{w'q_t'\theta_l'}$:

$$\frac{\overline{w'q_t'\theta_l'}}{(1-\tilde{\sigma}_w^2)^{1/2}(\overline{w'^2})^{1/2}(\overline{q_t'^2})^{1/2}(\overline{\theta_l'^2})^{1/2}} = \hat{c}_{wq_t}\hat{c}_{w\theta_l}\widehat{\mathrm{Sk}}_w + E(w, q_t, \theta_l)\frac{1}{2}\widehat{\mathrm{Sk}}_w(c_{q_t\theta_l} - \hat{c}_{wq_t}\hat{c}_{w\theta_l}), \tag{47}$$

$$\overline{w'q_t'\theta_l'} = \frac{\frac{1}{2}E}{(1-\tilde{\sigma}_w^2)}\overline{q_t'\theta_l'}\frac{\overline{w'^3}}{\overline{w'^2}} + \frac{1-\frac{1}{2}E}{(1-\tilde{\sigma}_w^2)^2}\overline{w'q_t'}\,\overline{w'\theta_l'}\frac{\overline{w'^3}}{(\overline{w'^2})^2}. \tag{48}$$

The function $E(w, q_t, \theta_l)$ is

$$E = \frac{1-\frac{1}{2}\frac{2a}{1-2a}\xi}{1+\frac{1}{2}\xi}, \tag{49}$$

where

$$1+\xi = \frac{1-a}{a}\frac{\tilde{\sigma}_{q_t2}}{\tilde{\sigma}_{q_t1}}\frac{\tilde{\sigma}_{\theta_l2}}{\tilde{\sigma}_{\theta_l1}} = \left(\frac{A_{q_t}-B_{q_t}}{-A_{q_t}-B_{q_t}}\right)^{1/2}\left(\frac{A_{\theta_l}-B_{\theta_l}}{-A_{\theta_l}-B_{\theta_l}}\right)^{1/2}, \tag{50}$$

and

$$A_{\theta_l} = \mathrm{Sk}_{\theta_l} - \frac{3}{2}\hat{c}_{w\theta_l}\widehat{\mathrm{Sk}}_w + \frac{1}{2}\hat{c}^3_{w\theta_l}\widehat{\mathrm{Sk}}_w, \tag{51}$$

$$B_{\theta l} = \frac{3}{2}(4 + \widehat{\mathrm{Sk}}^2_w)^{1/2}\hat{c}_{w\theta_l}(1 - \hat{c}^2_{w\theta_l}), \tag{52}$$

and A_{q_t} and B_{q_t} are analogous. We now list two cases in which the expression for E simplifies. First, if

$$\frac{\tilde{\sigma}_{q_{t2}}}{\tilde{\sigma}_{q_{t1}}}\frac{\tilde{\sigma}_{\theta_{t2}}}{\tilde{\sigma}_{\theta_{t1}}} = 1, \tag{53}$$

then $E = 0$. This would occur, for instance, if the widths of plumes 1 and 2 were equal to each other for both q_t and θ_t, that is, if $\tilde{\sigma}_{q_{t2}} = \tilde{\sigma}_{q_{t1}}$ and $\tilde{\sigma}_{\theta_{t2}} = \tilde{\sigma}_{\theta_{t1}}$. Second, if we use the diagnostic ansatz (33) for the scalar skewnesses, then

$$\xi = \frac{1 - 2\zeta}{\zeta}, \tag{54}$$

where

$$\zeta = a + \frac{1}{3}\beta(1 - 2a). \tag{55}$$

Then we find

$$E = \frac{2}{3}\beta. \tag{56}$$

5. What moments lead to a realizable Gaussian-mixture PDF?

In the assumed PDF method, the host model prognoses a set of moments, for example, $\overline{w}$, $\overline{q_t}$, $\overline{w'^2}$, etc. This set of moments may possess a property called "realizability." More precisely, one can introduce and define several varieties of realizability.

The assumed PDF method uses a set of prognosed moments to determine a PDF. But because the prognosed moments may contain errors, the set of moments may not correspond to any real PDF, that is, a PDF that is normalized and nonnegative everywhere (Pope 2000, p. 464). For instance, the host model may produce a negative variance. We call all such sets of moments "generically unrealizable." All other sets of moments, namely, each set that corresponds to some real PDF, we call "generically realizable."

A related but different case arises when a set of moments corresponds to a real PDF, but that PDF is not a member of the family of assumed PDFs. In other words, the set of moments is generically realizable but is unrealizable with respect to a particular assumed PDF family. Consider an example. Suppose that the assumed PDF family is a single Gaussian, which, by definition, has zero skewness. Furthermore, suppose that a host model prognoses a set of moments that includes a nonzero skewness. This set of moments does not correspond to any single Gaussian, although it may or may not correspond to a real PDF. We call all such sets of moments "specifically unrealizable" with respect to the PDF family of interest. In contrast, we call all other sets of moments, namely, those that correspond to a PDF within the PDF family of interest, "specifically realizable," or, more succinctly, "realizable" with respect to the PDF family. The terms "specifically realizable" and "specifically unrealizable" only have meaning if a particular PDF family is specified. Our definitions of realizability are not directly related to the moment inequalities presented in Zilitinkevich et al. (1999) and Abdella and Petersen (2000), which are approximate and do not pertain solely to a specific PDF family. Pope (2000) discusses generic realizability but not specific realizability.

A Venn diagram illustrating the relationship between these kinds of realizability is given in Fig. 2. The sets of moments that are generically unrealizable and the sets that are generically realizable are disjoint. Also disjoint are the sets of moments that are specifically unrealizable and specifically realizable with respect to the PDF

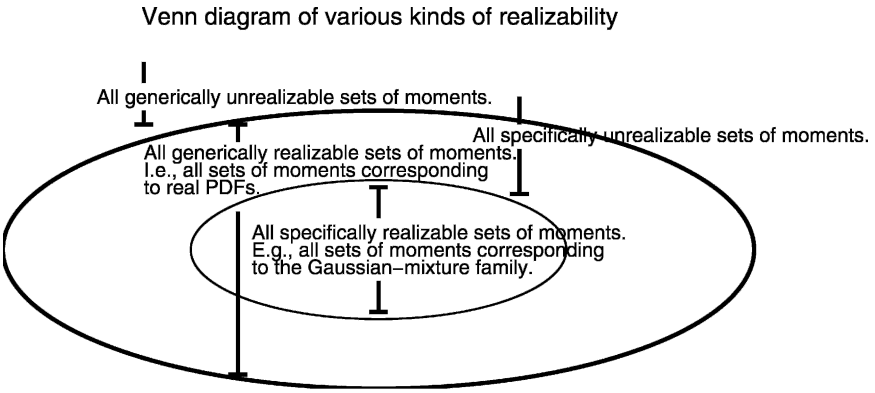

FIG. 2. A Venn diagram that illustrates types of realizability. Specific realizability is a subset of generic realizability. Generic realizability and generic unrealizability are mutually exclusive, as are specific realizability and specific unrealizability.

family of interest. The sets of moments that are specifically realizable with respect to the PDF family of interest form a subset of the generically realizable sets. It is advantageous to choose a PDF family that is broad, so that there are few sets of moments that are generically realizable but are specifically unrealizable with respect to the PDF family.

There are plausible sets of moments that are specifically unrealizable with respect to the Analytic Double Gaussian 1 family of Larson et al. (2002), because this PDF family is too restrictive. In particular, their skewness diagnoses, $\mathrm{Sk}_{\theta_l} = 0$ and $\mathrm{Sk}_{q_t} = 1.2\mathrm{Sk}_w$, can lead to negative or infinite values of $\tilde{\sigma}_{\theta_l 1,2}$ when $\hat{c}_{w\theta_l}$ and $\hat{c}_{wq_t}$ vanish [see Eqs. (26) and (27)]. When this happens in a numerical simulation, $\tilde{\sigma}_{\theta_l 1,2}$ must be reset to reasonable values (Larson et al. 2002).

This problem is ameliorated by the new mixture of trivariate Gaussians with scalar skewness given by (33) and plume w width given by (37). For realizability we require three conditions on the moments provided by the host model. First, the variances must be positive, that is,

$$\overline{w'^2}, \overline{\theta_l'^2}, \overline{q_t'^2} > 0. \tag{57}$$

Second, correlations must lie in the range $(-1, 1)$, that is,

$$-1 < c_{w\theta_l}, c_{wq_t}, c_{q_t\theta_l} < 1. \tag{58}$$

These two restrictions are not imposed by our assumed PDF family; any set of moments that violates these requirements is generically unrealizable. If we stipulate that $0 \le \gamma < 1$, then we see from (37), (16), and (17) that $-1 < \hat{c}_{w\theta_l}, \hat{c}_{wq_t} < 1$. If we combine this restriction on $\hat{c}_{w\theta_l}, \hat{c}_{wq_t}$ with the demand that $0 \le \beta \le 3$, then Eqs. (34) and (35) show that $\sigma^2_{\theta_l 1,2} > 0$, as required for realizability. Similarly, $\sigma^2_{q_t 1,2} > 0$.

There is a final requirement for realizability, namely, that $-1 < r_{q_t\theta_l} < 1$. (Recall that $r_{q_t\theta_l}$ is the subplume correlation; $c_{q_t\theta_l}$ is the total correlation.) To meet this requirement, (36) shows that for specific realizability with respect to the Gaussian-mixture PDF, we need

$$\hat{c}_{wq_t}\hat{c}_{w\theta_l} - (1 - \hat{c}^2_{wq_t})^{1/2}(1 - \hat{c}^2_{w\theta_l})^{1/2} < c_{q_t\theta_l} < \hat{c}_{wq_t}\hat{c}_{w\theta_l} + (1 - \hat{c}^2_{wq_t})^{1/2}(1 - \hat{c}^2_{w\theta_l})^{1/2}. \tag{59}$$

This condition is particular to our PDF, and not general to all PDFs. However, the condition is fairly unrestrictive, and many PDFs of practical interest satisfy it. For instance, this condition is violated by less than 1% of the LES PDFs of the Barbados Oceanographic and Meteorological Experiment (BOMEX), the First International Satellite Cloud Climatology Project (ISCCP) Regional Experiment (FIRE), and Wangara cases examined in this paper, when $\beta = 0.8$ and $\gamma = 0.45$. The range of acceptable values of $c_{q_t\theta_l}$ is centered on $\hat{c}_{wq_t}\hat{c}_{w\theta_l}$ and extends a distance $\pm(1 - \hat{c}^2_{wq_t})^{1/2}(1 - \hat{c}^2_{w\theta_l})^{1/2}$. When $\hat{c}_{wq_t} = \hat{c}_{w\theta_l} = 0$, the range of acceptable values is ± 1; when $\hat{c}_{wq_t} = \pm 1$ or $\hat{c}_{w\theta_l} = \pm 1$, there is only one acceptable value, namely, $c_{q_t\theta_l} = \hat{c}_{wq_t}\hat{c}_{w\theta_l}$. Every trivariate PDF family must have some restriction on the possible relationships between correlations—a set of three correlations cannot vary arbitrarily. To illustrate this, note that if w and θ_l are perfectly correlated, then q_t cannot be perfectly correlated with w but perfectly anticorrelated with θ_l.

To use this closure, a model code must enforce the realizability conditions (57), (58), and (59) by resetting the offending moment inputs to lie within the acceptable range. A negative or zero variance must be reset to a small, positive value. Likewise, unacceptable values of the correlations must be reset to lie within the ranges given by (58) and (59).

6. For comparison: Moment closures based on the double delta function PDF

In this section we describe an alternative PDF that consists of two delta functions. A double delta function PDF corresponds to a two-plume mass-flux scheme that contains no within-plume variability (Randall et al. 1992; de Roode et al. 2000; Lappen and Randall 2001). We compute the PDF parameters following Randall et al. (1992). In this method, one positions the delta functions such that the PDF matches the scalar fluxes $\overline{w'\theta_l'}$ and $\overline{w'q_t'}$. Then the scalar variances, $\overline{\theta_l'^2}$ and $\overline{q_t'^2}$, are not guaranteed to be matched. An alternative is to match the scalar variances, but then the scalar fluxes are not necessarily matched. This alternative PDF family is not investigated here.

The double delta PDF family is a special case of the trivariate mixture of Gaussians in which the widths of the individual plumes tend to zero. The analogy is highlighted by the hat notation used above. The similarity shows that the Gaussian-mixture PDF is as simple as the double delta PDF in some respects (but not all).

a. Functional form of the mixture of two delta functions

The functional form is

$$\sqrt{\overline{w'^2}\,\overline{\theta_l'^2}\,\overline{q_t'^2}}P_{dd} = a\delta(\hat{w}' - \hat{w}_1)\delta(\tilde{\theta}_l' - \tilde{\theta}_{l1})\delta(\tilde{q}_t' - \tilde{q}_{t1}) + (1 - a)\delta(\hat{w}' - \hat{w}_2)\delta(\tilde{\theta}_l' - \tilde{\theta}_{l2})\delta(\tilde{q}_t' - \tilde{q}_{t2}). \tag{60}$$

Here δ denotes the Dirac delta function.

b. A list of given moments and PDF parameters

To use the double delta function PDF, one would need to prognose the following seven moments: $\overline{w}$, $\overline{w'^2}$, $\overline{w'^3}$, $\overline{\theta_l}$, $\overline{w'\theta_l'}$, $\overline{q_t}$, and $\overline{w'q_t'}$.

These moments could then be used to specify the seven PDF parameters: a, $\hat{w}_1$, $\hat{w}_2$, $\tilde{\theta}_{l1}$, $\tilde{\theta}_{l2}$, $\tilde{q}_{t1}$, and $\tilde{q}_{t2}$.

c. Writing given moments in terms of PDF parameters

To convert from PDF parameters to moments, we set $\tilde{\sigma}_w = \tilde{\sigma}_{\theta l1} = \tilde{\sigma}_{\theta_l 2} = \tilde{\sigma}_{q_t 1} = \tilde{\sigma}_{q_t 2} = 0$, and use Eqs. (9), (10), (11), (12), (14), (16), and (17).

d. Finding PDF parameters in terms of moments

To solve for the PDF parameters, we set $\tilde{\sigma}_w^2 = 0$, which implies that we drop all hats, ^. Then we use Eqs. (20)–(25).

e. Closures for third- and fourth-order moments based on the mixture of delta functions

Formulas for Sk_{θ_l}, $\overline{w'^4}$, $\overline{w'^2\theta_l'}$, $\overline{w'\theta_l'^2}$, and $\overline{w'q_t'\theta_l'}$ based on the double delta family can be recovered from the Gaussian-mixture family by setting $E = \beta = 0$ and $\tilde{\sigma}_w^2 = 0$ in Eqs. (33), (39), (41), (43), and (47). The latter change means that all hats $\widehat{()}$ can be dropped from the formulas. We find the following formulas. For the scalar skewness, the double delta function yields

$$\mathrm{Sk}_{\theta_l} = \mathrm{Sk}_w c_{w\theta_l}^3. \tag{61}$$

It is important to note that for the double delta PDF, Sk_{θ_l} and Sk_{q_t} are not free parameters that can be prognosed or diagnosed, as for the Gaussian-mixture PDF [see Eq. (33)]. Rather, for the double delta PDF, the scalar skewnesses are determined by the choices of Sk_w and the scalar fluxes. From (61) we see that Sk_{θ_l} is much smaller than Sk_w when $c_{w\theta_l}$ is moderately less than unity.[2]

The double delta PDF yields the following formula for $\overline{w'^4}$ [see, e.g., Gryanik and Hartmann 2002, their Eq. (13)]:

$$\frac{\overline{w'^4}}{\overline{w'^2}\,\overline{w'^2}} = 1 + \mathrm{Sk}_w^2. \tag{62}$$

When $\mathrm{Sk}_w = 0$, this reduces to a smaller value, 1, than for a single Gaussian, 3. In addition, the double delta function yields

$$\frac{\overline{w'^2\theta_l'}}{\overline{w'^2}(\overline{\theta_l'^2})^{1/2}} = c_{w\theta_l}\mathrm{Sk}_w. \tag{63}$$

This formula was proposed by Abdella and McFarlane (1997), Zilitinkevich et al. (1999), and Gryanik and Hartmann (2002). The double delta PDF also gives

$$\frac{\overline{w'\theta_l'^2}}{(\overline{w'^2})^{1/2}\overline{\theta_l'^2}} = c_{w\theta_l}^2\mathrm{Sk}_w = \frac{\mathrm{Sk}_{\theta_l}}{c_{w\theta_l}}. \tag{64}$$

This differs from the mass-flux formulas of Mironov et al. (1999), Abdella and Petersen (2000), and Gryanik and Hartmann (2002), who instead propose a formula that can be derived from a triple delta function PDF. Finally, we find

$$\frac{\overline{w'q_t'\theta_l'}}{(\overline{w'^2})^{1/2}(\overline{q_t'^2})^{1/2}(\overline{\theta_l'^2})^{1/2}} = c_{wq_t}c_{w\theta_l}\mathrm{Sk}_w. \tag{65}$$

7. For comparison: Moment closures based on the triple delta function PDF

To formulate a closure for $\overline{w'\theta_l'^2}$, one could simply switch the role of w and θ_l in the double delta closure for $\overline{w'^2\theta_l'}$ (63). This yields

$$\frac{\overline{w'\theta_l'^2}}{(\overline{w'^2})^{1/2}\overline{\theta_l'^2}} = c_{w\theta_l}\mathrm{Sk}_{\theta_l}. \tag{66}$$

This formula is valid; in fact, it fits the LES in Figs. 3–8 better than the double delta Eq. (64). However, (66) is not consistent with the double delta PDF family, as shown by comparison with (64). Rather, (66) is consistent with a triple delta PDF family (see Mironov et al. 1999; Gryanik and Hartmann 2002). We will define this PDF in this section. In accordance with prior authors, we consider for simplicity only a bivariate triple delta PDF in w and θ_l. This section concludes with sample plots of the triple delta, double delta, and Gaussian-mixture PDFs.

a. Functional form of the mixture of three delta functions

We define two mixture fractions: the velocity ($\hat{w}$) mixture fraction is governed by $-1 < a < 1$; and the temperature ($\tilde{\theta}_l$) mixture fraction is governed by $-1 < b < 1$. We have two cases. When $b \geq a$, the delta functions are located at $(\hat{w}_1, \tilde{\theta}_{l1})$, $(\hat{w}_2, \tilde{\theta}_{l1})$, and $(\hat{w}_2, \tilde{\theta}_{l2})$. The PDF is

$$\begin{aligned}\sqrt{\overline{w'^2}\,\overline{\theta_l'^2}}P_{td} = {} & a\delta(\hat{w}' - \hat{w}_1)\delta(\tilde{\theta}_l' - \tilde{\theta}_{l1}) + (b - a)\delta(\hat{w}' \\ & - \hat{w}_2)\delta(\tilde{\theta}_l' - \tilde{\theta}_{l1}) + (1 - b)\delta(\hat{w}' \\ & - \hat{w}_2)\delta(\tilde{\theta}_l' - \tilde{\theta}_{l2}).\end{aligned} \tag{67}$$

When $a \geq b$, the delta functions are located at $(\hat{w}_1, \tilde{\theta}_{l1})$, $(\hat{w}_1, \tilde{\theta}_{l2})$, and $(\hat{w}_2, \tilde{\theta}_{l2})$. The PDF is

$$\begin{aligned}\sqrt{\overline{w'^2}\,\overline{\theta_l'^2}}P_{td} = {} & b\delta(\hat{w}' - \hat{w}_1)\delta(\tilde{\theta}_l' - \tilde{\theta}_{l1}) + (a - b)\delta(\hat{w}' \\ & - \hat{w}_1)\delta(\tilde{\theta}_l' - \tilde{\theta}_{l2}) + (1 - a)\delta(\hat{w}' \\ & - \hat{w}_2)\delta(\tilde{\theta}_l' - \tilde{\theta}_{l2}).\end{aligned} \tag{68}$$

[2] One might expect $c_{w\theta_l} = \pm 1$ always for a double delta function. Recall, however, that with the double delta function of Randall et al. (1992), the scalar variances of the PDF do not in general match those of the true PDF. Since we define the correlation $c_{w\theta_l}$ in terms of the true $\overline{\theta_l'^2}$ rather than the double delta's diagnosis of $\overline{\theta_l'^2}$, it is possible to have $|c_{w\theta_l}| < 1$. For an example in which the double delta function of Randall et al. (1992) diagnoses $Sk_{\theta_l} = \overline{w'\theta_l'} = 0$, see the lower-right panel of Fig. 1.

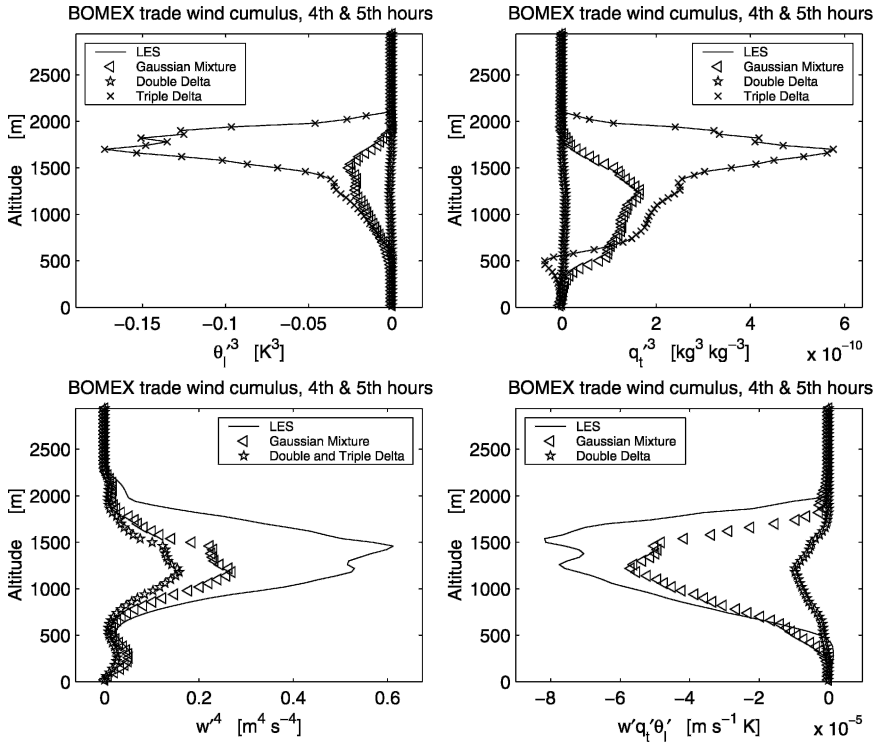

FIG. 3. Profiles of $\overline{\theta_l'^3}$, $\overline{q_t'^3}$, $\overline{w'^4}$, and $\overline{w'q_t'\theta_l'}$ for the BOMEX trade wind cumulus simulation, time averaged over the fourth and fifth hours. Shown are LES output (–), approximations based on the mixture of two trivariate Gaussians PDF (triangles), and approximations based on double delta (stars) and triple delta (x) function PDFs. For $\overline{w'^4}$, the double delta and triple delta PDFs yield the same formula. For the Gaussian-mixture PDF, we choose $\beta = 0.8$ and $\gamma = 0.45$, where $\tilde{\sigma}_w^2 = \gamma[1 - \max(c_{w\theta_l}^2, c_{wq_t}^2)]$. The Gaussian-mixture PDF tends to underpredict the moments, and the double delta PDF does so more severely.

Thus the three delta functions are located at the corners of a right triangle in $(\hat{w}, \tilde{\theta}_l)$ space (see Fig. 1, discussed below). Each delta function represents one plume. For example, in addition to having a warm-updraft and cold-downdraft plume, a triple delta could also include a cold-updraft plume.

b. A list of given moments and PDF parameters

The bivariate triple delta function requires as input six moments: $\overline{w}$, $\overline{w'^2}$, $\overline{w'^3}$, $\overline{\theta_l}$, $\overline{\theta_l'^2}$, and $\overline{\theta_l'^3}$. These moments can then be used to specify the six PDF parameters: a, b, $\hat{w}_1$, $\hat{w}_2$, $\tilde{\theta}_{l1}$, and $\tilde{\theta}_{l2}$. The triple delta PDF does not satisfy the turbulent flux, $\overline{w'\theta_l'}$, unlike the Gaussian-mixture or double delta PDF families. However, the triple delta does satisfy $\overline{\theta_l'^3}$.

c. Writing moments in terms of PDF parameters

These equations are listed in dimensional form by Gryanik and Hartmann (2002). The dimensionless form is, for $b \geq a$,

$$\frac{\overline{w'^n\theta_l'^m}}{(\overline{w'^2})^{n/2}(\overline{\theta_l'^2})^{m/2}} = a(\hat{w}_1)^n(\tilde{\theta}_{l1})^m + (b - a)(\hat{w}_2)^n(\tilde{\theta}_{l1})^m + (1 - b)(\hat{w}_2)^n(\tilde{\theta}_{l2})^m. \quad (69)$$

For $a \geq b$,

$$\frac{\overline{w'^n\theta_l'^m}}{(\overline{w'^2})^{n/2}(\overline{\theta_l'^2})^{m/2}} = b(\hat{w}_1)^n(\tilde{\theta}_{l1})^m + (a - b)(\hat{w}_1)^n(\tilde{\theta}_{l2})^m + (1 - a)(\hat{w}_2)^n(\tilde{\theta}_{l2})^m. \quad (70)$$

d. Finding PDF parameters in terms of moments

To solve for a, $\hat{w}_1$, and $\hat{w}_2$, we use Eqs. (20), (21), and (22) and set $\tilde{\sigma}_w^2 = 0$. To solve for b, $\tilde{\theta}_{l1}$, and $\tilde{\theta}_{l2}$, we use the same equations (with $\tilde{\sigma}_w^2 = 0$), but we replace a by b and w by θ_l everywhere.

e. Closures for third- and fourth-order moments based on the mixture of delta functions

The triple delta function leads to the same formulas as the double delta function for $\overline{w'^4}$ (62) and $\overline{w'^2\theta_l'}$ (63). For $\overline{w'\theta_l'^2}$, in contrast, the triple delta yields (66). Since we have formulated the triple delta as a bivariate PDF, we cannot find a formula for the trivariate moment $\overline{w'q_t'\theta_l'}$.

We plot examples of the Gaussian-mixture, double delta, and triple delta PDFs in Fig. 1. This figure illus-

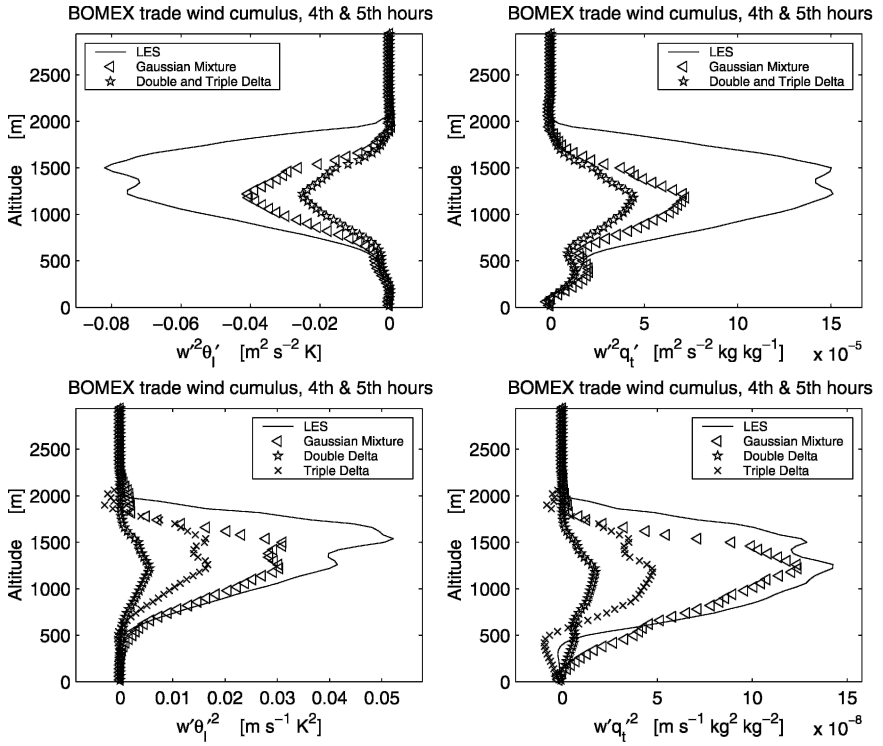

FIG. 4. Profiles of $\overline{w'^2\theta_l'}$, $\overline{w'^2q_t'}$, $\overline{w'\theta_l'^2}$, and $\overline{w'q_t'^2}$ for the BOMEX trade wind cumulus simulation, time averaged over the fourth and fifth hours. Shown are LES output (—), approximations based on the mixture of two trivariate Gaussians PDF (triangles), and approximations based on double delta (stars) and triple delta (x) function PDFs. For $\overline{w'^2\theta_l'}$ and $\overline{w'^2q_t'}$, the double delta and triple delta PDFs yield the same formula. For the Gaussian-mixture PDF, we choose $\beta = 0.8$ and $\gamma = 0.45$, where $\tilde{\sigma}_w^2 = \gamma[1 - \max(c_{w\theta_l}^2, c_{wq_t}^2)]$. All three PDFs underpredict the moments, the Gaussian-mixture least severely and the double delta most severely.

trates how Gaussian-mixture PDFs look if we make the assumption, embodied in (33), that Sk_w and Sk_{θ_l} have the same sign when $\overline{w'\theta_l'} > 0$ (i.e., $c_{w\theta_l} > 0$) and vice versa for $\overline{w'\theta_l'} < 0$. This assumption is reasonable but not always true. Consider now the delta function PDFs. Although the double delta PDF captures the variability in w, the delta functions are too closely spaced in θ_l. This is especially notable in the lower-right panel, where w and θ_l are uncorrelated. In contrast, the triple delta function captures variability in both w and θ_l. Neither the double nor triple delta functions are able to sample the extremities or tails of a spread-out distribution.

8. How well do the closures model LES output?

In this section we compare closures for higher-order moments versus output from LESs. We consider clear, cumulus, and stratocumulus boundary layers. The closures are based on the Gaussian-mixture, double delta, and triple delta PDFs.

The first case that we simulate, BOMEX (Siebesma et al. 2003), is a trade wind cumulus case. The second case is a nocturnal stratocumulus-topped boundary layer, based on FIRE (Moeng et al. 1996). The third case is a clear convective boundary layer, based on day 33 of the Wangara experiment (Clarke et al. 1971; Deardorff 1974; André et al. 1978).

The LES model is the Regional Atmospheric Modeling System (RAMS), version 4.2x (Cotton et al. 2003). Liquid water is diagnosed using a saturation adjustment scheme that instantly evaporates liquid in subsaturated air and instantly condenses liquid in supersaturated air. Otherwise, all microphysics is turned off. The horizontal grid spacing is 50 m for the FIRE case and 100 m for BOMEX and Wangara. The simulations have periodic horizontal boundary conditions and a flat lower surface. The BOMEX and FIRE cases were set up according to specifications from Global Energy and Water Experiment (GEWEX) Cloud System Study (GCSS) intercomparisons. RAMS simulations compare well with those of other models. The Wangara case has not been compared by GCSS; however, our simulation agreed with field observations. Details of the setup of the cases are listed in Golaz et al. (2002b) and references therein.

We overplot higher-order moments computed from the LES with moments approximated by the PDF fami-

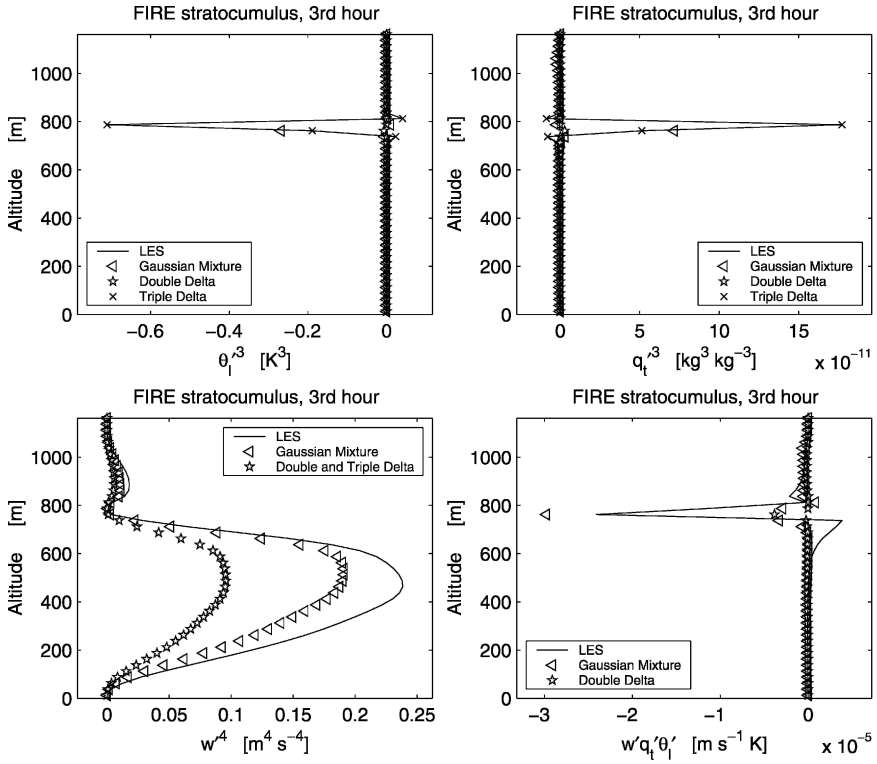

FIG. 5. Profiles of $\overline{\theta_l'^3}$, $\overline{q_t'^3}$, $\overline{w'^4}$, and $\overline{w'q_t'\theta_l'}$ for the FIRE stratocumulus simulation, time averaged over the third hour. Shown are LES output (–), approximations based on the mixture of two trivariate Gaussians PDF (triangles), and approximations based on double delta (stars) and triple delta (x) function PDFs. For $\overline{w'^4}$, the double delta and triple delta PDFs yield the same formula. For the Gaussian-mixture PDF, we choose $\beta = 0.8$ and $\gamma = 0.45$, where $\tilde{\sigma}_w^2 = \gamma[1 - \max(c_{w\theta_l}^2, c_{wq_t}^2)]$. For $\overline{\theta_l'^3}$, $\overline{q_t'^3}$, and $\overline{w'^4}$, the Gaussian-mixture PDF tends to underpredict the moments, and the double delta PDF does so more severely.

lies. To calculate the approximations to higher-order moments, we obtain the needed lower-order moments directly from the LES. Thus our comparison with LES is diagnostic. A test of how well the moments perform in an interactive one-dimensional higher-order closure model will be deferred to a forthcoming manuscript.

The moments we plot are $\overline{\theta_l'^3}$, $\overline{q_t'^3}$, $\overline{w'^4}$, $\overline{w'q_t'\theta_l'}$, $\overline{w'^2\theta_l'}$, $\overline{w'^2q_t'}$, $\overline{w'\theta_l'^2}$, and $\overline{w'q_t'^2}$. The Gaussian-mixture approximations we plot are given in Eqs. (38), (40), (48) with $E = (2/3)\beta$, (42), and (46). The corresponding double delta approximations are given by the same equations, but with $\tilde{\sigma}_w^2 = \beta = E = 0$. The triple delta approximations for $\overline{w'^4}$ and $\overline{w'^2\theta_l'}$ are the same as those for the double delta. The triple delta formula for $\overline{w'\theta_l'^2}$ is (66). The triple delta PDF satisfies $\overline{\theta_l'^3}$ exactly by construction. Formulas for $\overline{w'q_t'^2}$ and $\overline{w'^2q_t'}$ are analogous to those for $\overline{w'\theta_l'^2}$ and $\overline{w'^2\theta_l'}$. Since our triple delta PDF is bivariate, it cannot approximate the trivariate moment $\overline{w'q_t'\theta_l'}$; thus, it is not plotted.

The higher-order moments are plotted in Figs. 3–8. All three approximations we test have shortcomings. Of the three, however, the Gaussian-mixture PDF performs the best overall, and the double delta PDF performs worst.

Considering all three cases overall, the Gaussian-mixture PDF tends to underpredict $\overline{\theta_l'^3}$ and $\overline{q_t'^3}$, and in some instances overpredict $\overline{w'\theta_l'^2}$, $\overline{w'q_t'^2}$, and $\overline{w'q_t'\theta_l'}$. This occurs especially near the top of the boundary layer, where the scalar fluxes, $\overline{w'\theta_l'}$ and $\overline{w'q_t'}$, are small. This is because $\overline{\theta_l'^3}$ and $\overline{q_t'^3}$ are proportional to the scalar fluxes [see Eq. (38)], but $\overline{w'\theta_l'^2}$, $\overline{w'q_t'^2}$, and $\overline{w'q_t'\theta_l'}$ are not [see Eq. (46)]. In the BOMEX case, the Gaussian-mixture underpredicts everything except $\overline{w'q_t'^2}$; in the FIRE and Wangara cases, it underpredicts some moments and overpredicts others.

In Figs. 3–8, we have set $\beta = 0.8$ and $\gamma = 0.45$. Other values may be more appropriate for other cases. Depending on the situation, changes in these parameters can affect the results strongly or weakly; for our cases, the sensitivity is moderate. An increase in β leads to larger $|\overline{\theta_l'^3}|$, $|\overline{q_t'^3}|$, $|\overline{w'\theta_l'^2}|$, and $|\overline{w'q_t'^2}|$; leaves unchanged $\overline{w'^4}$, $\overline{w'^2\theta_l'}$, and $\overline{w'^2q_t'}$; and can either increase or decrease $|\overline{w'q_t'\theta_l'}|$. An increase in γ tends to increase the magnitudes of all plotted moments, for typical parameter values. Formulas for the sensitivities are presented in appendix B.

How much error is introduced in the Gaussian-mixture PDF by diagnosing scalar skewnesses via (33)

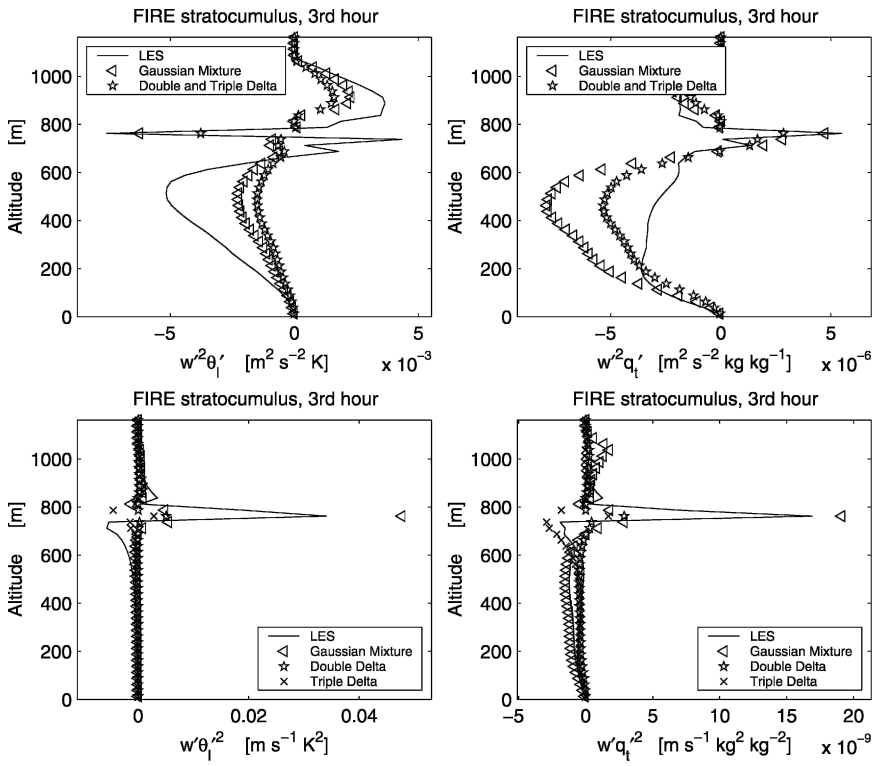

FIG. 6. Profiles of $\overline{w'^2\theta_l'}$, $\overline{w'^2q_t'}$, $\overline{w'\theta_l'^2}$, and $\overline{w'q_t'^2}$ for the FIRE stratocumulus simulation, time averaged over the third hour. Shown are LES output (–), approximations based on the mixture of two trivariate Gaussians PDF (triangles), and approximations based on double delta (stars) and triple delta (x) function PDFs. For $\overline{w'^2\theta_l'}$ and $\overline{w'^2q_t'}$, the double delta and triple delta PDFs yield the same formula. For the Gaussian-mixture PDF, we choose $\beta = 0.8$ and $\gamma = 0.45$, where $\tilde{\sigma}_w^2 = \gamma[1 - \max(c_{w\theta_l}^2, c_{wq_t}^2)]$. The Gaussian-mixture provides a better fit for $\overline{w'^2\theta_l'}$, $\overline{w'\theta_l'^2}$, and $\overline{w'q_t'^2}$; the double/triple delta performs better for $\overline{w'^2q_t'}$.

rather than prognosing them? How much error is introduced by prohibiting nonzero within-plume velocity–scalar correlations? These questions were addressed by Larson et al. (2002), who investigated the closure of Lewellen and Yoh (1993), which relaxes these restrictions. Larson et al. (2002) found that the Lewellen–Yoh closure can lead to moderate improvements. Unfortunately for the present paper's objectives, the Lewellen–Yoh closure is not analytic.

The double delta function PDF underpredicts all moments except $\overline{w'^2q_t'}$ in FIRE. Prior research (and Fig. 1) shows that the variant of double delta function studied here, which matches scalar fluxes, tends to underpredict scalar variances (Wang and Stevens 2000; Larson et al. 2002). Also severely underpredicted are $\overline{\theta_l'^3}$ and $\overline{q_t'^3}$. This is not surprising, given that $\overline{\theta_l'^3} \propto c_{w\theta_l}^3$, and $|c_{w\theta_l}| < 1$. Analogous expressions hold for q_t.

In contrast, the triple delta PDF satisfies $\overline{\theta_l'^3}$ and $\overline{q_t'^3}$ exactly. However, the triple delta underpredicts $\overline{w'^4}$, $\overline{w'^2\theta_l'}$, and $\overline{w'^2q_t'}$, since for these moments it yields the same approximations as the double delta PDF. The triple delta also underpredicts $\overline{w'\theta_l'^2}$ and $\overline{w'q_t'^2}$, although not as severely in BOMEX as does the double delta.

9. Conclusions

This paper discusses a methodology for deriving closures of higher-order moments in terms of lower- or equal-order moments. The procedure involves assuming a functional form of a family of probability density functions (PDFs). The method has been used previously by meteorologists who assumed that the PDF family is a double or triple delta function (Randall et al. 1992; Abdella and McFarlane 1997; Zilitinkevich et al. 1999; Mironov et al. 1999; Abdella and Petersen 2000; Lappen and Randall 2001; Gryanik and Hartmann 2002). Here we assume instead that the PDF is a mixture of two trivariate Gaussians, as given by Eqs. (4) and (5).

The assumed PDF method has several advantages. First, it can guarantee that if the lower-order moments are compatible with the assumed PDF family, then the higher-order moments obtained are specifically realizable, in the sense that they correspond to a member of the family of assumed PDFs. In particular, our Gaussian-mixture closures guarantee realizability in this sense if the variances are positive, correlations range between -1 and 1, and if Eq. (59) holds among the

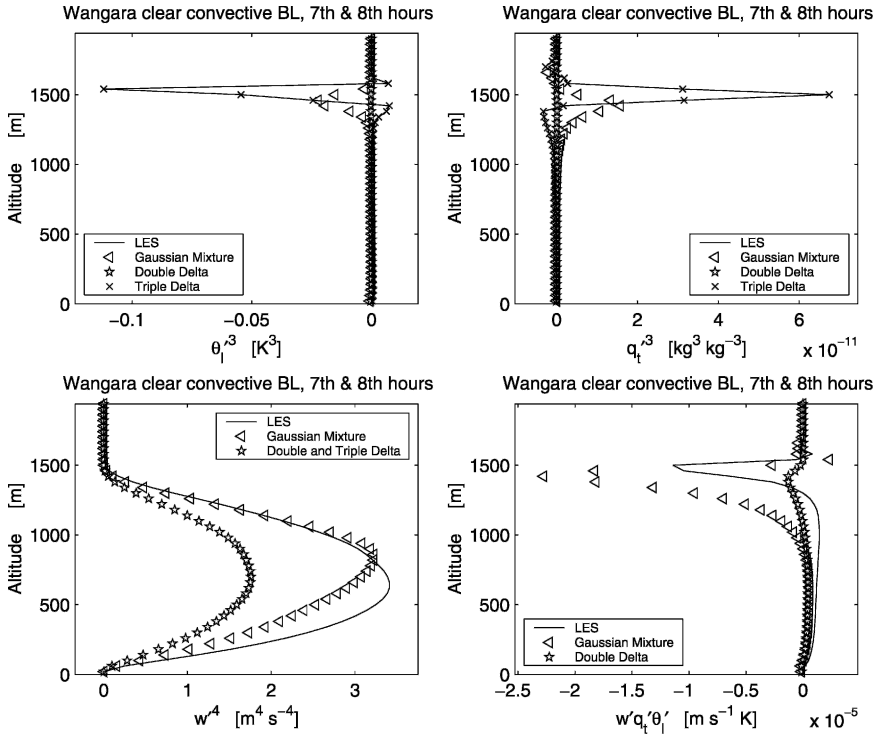

FIG. 7. Profiles of $\overline{\theta_l'^3}$, $\overline{q_t'^3}$, $\overline{w'^4}$, and $\overline{w'q_t'\theta_l'}$ for the Wangara clear convective boundary layer simulation, time averaged over the seventh and eighth hours. Shown are LES output (–), approximations based on the mixture of two trivariate Gaussians PDF (triangles), and approximations based on double delta (stars) and triple delta (x) function PDFs. For $\overline{w'^4}$, the double delta and triple delta PDFs yield the same formula. For the Gaussian-mixture PDF, we choose $\beta = 0.8$ and $\gamma = 0.45$, where $\tilde{\sigma}_w^2 = \gamma[1 - \max(c_{w\theta_l}^2, c_{wq_t}^2)]$. The Gaussian-mixture PDF underpredicts $\overline{\theta_l'^3}$ and $\overline{q_t'^3}$, but overpredicts $\overline{w'q_t'\theta_l'}$. The double delta PDF underpredicts all moments.

correlations. Second, the assumed PDF method ensures that the higher-order closure formulas are consistent with one another, in the sense that they are all derived from the same PDF. This is useful because often many closure moments must be derived. Third, the assumed PDF method helps us derive moment relations with the correct parity, or reflectional symmetry. In our case, this leads to closures that are equally valid for both upward and downward scalar fluxes. Finally, the method provides a physical interpretation of the coefficients that appear in the closure, since these coefficients are directly related to the shape of the assumed PDF.

This paper contains two main results. The first is the diagnostic Eq. (33) for scalar skewness, Sk_{θ_l} or Sk_{q_t}, in terms of vertical velocity skewness, Sk_w. Equation (33) has been postulated; it is not derived from an assumption of a Gaussian-mixture PDF. The formula is independent of the Gaussian-mixture PDF, although we use it in conjunction with the Gaussian-mixture PDF. The formula's chief virtues are that it is simple and physically plausible. However, it does tend to underpredict scalar skewness in the boundary layer cases we tested (see Figs. 3, 5, and 7) for parameter values that fit the other third-order moments well.

The second main result is simple, analytic closures for $\overline{w'^4}$(40), $\overline{w'q_t'\theta_l'}$(48), $\overline{w'^2\theta_l'}$(42), $\overline{w'\theta_l'^2}$ (46), and analogous closures for $\overline{w'^2q_t'}$ and $\overline{w'q_t'^2}$. If we assume $E = (2/3)\beta$ [see Eq. (56)], then these closures are simple enough to be written down in a single line in terms of lower-order moments (as opposed to PDF parameters). These closures have been derived from the formula for scalar skewness (33) and the assumption of a Gaussian-mixture PDF. The closures depend on two parameters: the variance of the individual Gaussian plumes (components), $\tilde{\sigma}_w^2$, and a parameter β that governs the scalar skewnesses. Inspection of how $\tilde{\sigma}_w^2$ and β enter the formulas gives insight into how the moments change as the PDFs change shape.

The closures are compared with large eddy simulations in Figs. 3–8. Although the fits have shortcomings, they are superior in most cases we test to those based on double or triple delta function PDFs. Delta functions have difficulties essentially because introducing highly peaked functions into a PDF drastically alters its higher-order moments. The assumed PDF methodology can be used with any tractable PDF, and we hope that more sophisticated PDFs than any presented here will be used in the future to derive closures.

How well the Gaussian-mixture closures work in an interactive boundary layer parameterization has been

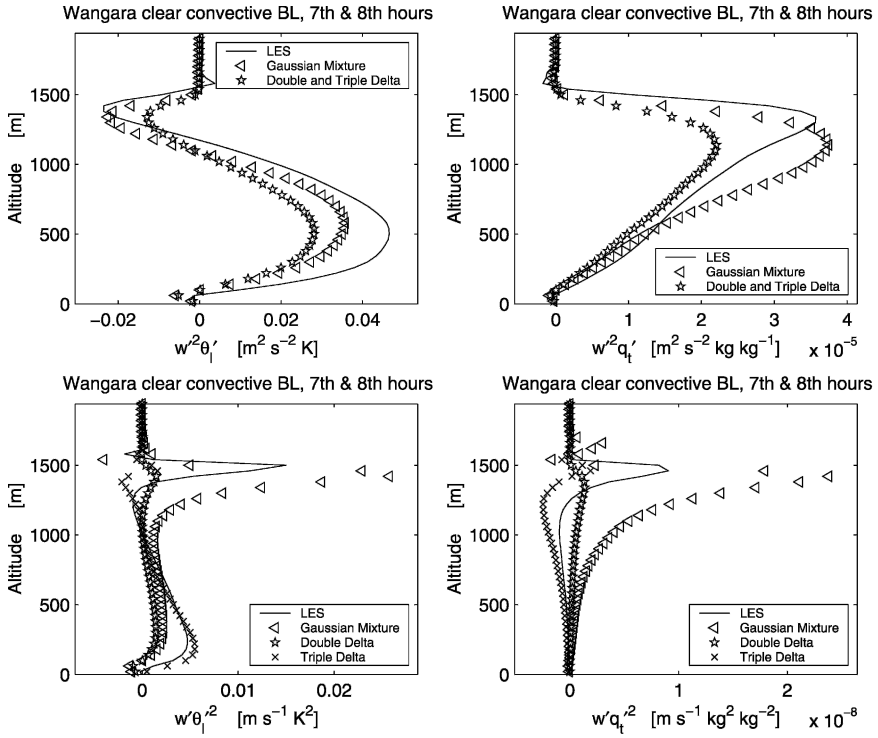

FIG. 8. Profiles of $\overline{w'^2\theta_l'}$, $\overline{w'^2q_t'}$, $\overline{w'\theta_l'^2}$, and $\overline{w'q_t'^2}$ for the Wangara clear convective boundary layer simulation, time averaged over the seventh and eighth hours. Shown are LES output (–), approximations based on the mixture of two trivariate Gaussians PDF (triangles), and approximations based on double delta (stars) and triple delta (x) function PDFs. For $\overline{w'^2\theta_l'}$ and $\overline{w'^2q_t'}$, the double delta and triple delta PDFs yield the same formula. For the Gaussian-mixture PDF, we choose $\beta = 0.8$ and $\gamma = 0.45$, where $\tilde{\sigma}_w^2 = \gamma[1 - \max(c_{w\theta_l}^2, c_{wq_t}^2)]$. The Gaussian-mixture PDF fits $\overline{w'\theta_l'^2}$ and $\overline{w'^2q_t'}$ poorly. For these moments, the triple delta PDF performs better, except near the inversion.

tested by implementing the closures in the one-dimensional model of Golaz et al. (2002a,b). The results will be presented in the future.

Acknowledgments. The first author is grateful for financial support provided by Grant ATM-0239982 from the National Science Foundation, and by subaward G-7424-1 from the DoD Center for Geosciences/Atmospheric Research at Colorado State University via Cooperative Agreement DAAD19-02-2-0005 with the Army Research Laboratory. This research was performed while the second author held a National Research Council Research Associateship Award at the Naval Research Laboratory, Monterey, California.

APPENDIX A

Summary of Major Notation

Symbol	Definition	Equation
$\overline{()}$	Grid-box-averaged value	—
$()'$	Deviation from grid-box-averaged value	—
$()_i$	A quantity corresponding to the ith "plume"	—
Moment variable	**Definition**	**Equation**
w	Vertical velocity	—
$\hat{w}'$	Normalized and centered w	(3)
Sk_w	Skewness of w	$\mathrm{Sk}_w = \overline{w'^3}/(\overline{w'^2})^{3/2}$
$\widehat{\mathrm{Sk}}_w$	Normalized skewness of w	$\widehat{\mathrm{Sk}}_w = \mathrm{Sk}_w(1 - \tilde{\sigma}_w^2)^{-3/2}$
θ_l	Liquid water potential temperature	—

Moment variable	Definition	Equation
$\tilde{\theta}_l'$	Normalized and centered θ_l	(1)
Sk_{θ_l}	Skewness of θ_l	$\mathrm{Sk}_{\theta_l} = \overline{\theta_l'^3}/(\overline{\theta_l'^2})^{3/2}$
q_t	Total specific water content	—
$\tilde{q}_t'$	Normalized and centered q_t	(2)
Sk_{q_t}	Skewness of q_t	$\mathrm{Sk}_{q_t} = \overline{q_t'^3}/(\overline{q_t'^2})^{3/2}$
$-1 < c_{w\theta_l} < 1$	Correlation of w and θ_l	(16)
$-1 < \hat{c}_{w\theta_l} < 1$	Normalized correlation of w and θ_l	$\hat{c}_{w\theta_l} = c_{w\theta_l}(1 - \tilde{\sigma}_w^2)^{-1/2}$
$-1 < c_{wq_t} < 1$	Correlation of w and q_t	(17)
$-1 < \hat{c}_{wq_t} < 1$	Normalized correlation of w and q_t	$\hat{c}_{wq_t} = c_{wq_t}(1 - \tilde{\sigma}_w^2)^{-1/2}$
$-1 < c_{q_t\theta_l} < 1$	Correlation of q_t and θ_l	(18)

PDF parameter	Definition	Equation
$0 < a < 1$	Mixture fraction	(4)
σ_w	Standard deviation in w of individual plumes	—
$\tilde{\sigma}_w$	Normalized σ_w	$\tilde{\sigma}_w = \sigma_w/\sqrt{\overline{w'^2}}$
$\sigma_{\theta_l i}$	Standard deviation in θ_l of ith plume	—
$\tilde{\sigma}_{\theta_l i}$	Normalized standard deviation in θ_l of ith plume	$\tilde{\sigma}_{\theta_l i} = \sigma_{\theta_l i}/\sqrt{\overline{\theta_l'^2}}$
$\sigma_{q_t i}$	Standard deviation in q_t of ith plume	—
$\tilde{\sigma}_{q_t i}$	Normalized standard deviation in q_t of ith plume	$\tilde{\sigma}_{q_t i} = \sigma_{q_t i}/\sqrt{\overline{q_t'^2}}$
$0 \le \beta \le 3$	Dimensionless parameter that governs scalar skewness	(33)
$0 \le \gamma < 1$	Dimensionless parameter that governs $\tilde{\sigma}_w^2$	(37)
$-1 < r_{q_t\theta_l} < 1$	Correlation of q_t and θ_l for ith plume	—
δ	Dirac delta function. Normalized function that is infinite when its argument vanishes and zero elsewhere.	

APPENDIX B

How Sensitive is the Gaussian-Mixture Closure to the Parameters γ and β?

It is of interest to determine how much the Gaussian-mixture higher-order moments vary with the adjustable parameters γ and β. Because the closure formulas can be derived analytically, we can compute these sensitivities simply by taking the appropriate partial derivatives. For instance, if we want to know the change in $\overline{w'^4}$, $\delta\overline{w'^4}$, arising from a change in γ, $\delta\gamma$, we simply compute $\delta\overline{w'^4} = (\partial\overline{w'^4}/\partial\gamma)\delta\gamma$.

The needed derivatives are presented here. In the following formulas, recall that $\tilde{\sigma}_w^2 = \gamma[1 - \max(c_{w\theta_l}^2, c_{wq_t}^2)]$. The formulas for $\overline{w'\theta_l'^2}$ and $\overline{w'q_t'\theta_l'}$ assume that we have substituted in the diagnostic ansatz for scalar skewness, (33).

$$\frac{\partial\overline{\theta_l'^3}}{\partial\gamma} = [1 - \max(c_{w\theta_l}^2, c_{wq_t}^2)]\frac{1}{(1-\tilde{\sigma}_w^2)^3}\frac{\overline{w'^3}}{(\overline{w'^2})^2}\overline{\theta_l'^2}\,\overline{w'\theta_l'}\left(2\beta + 3(1-\beta)\frac{1}{1-\tilde{\sigma}_w^2}\frac{(\overline{w'\theta_l'})^2}{\overline{w'^2}\,\overline{\theta_l'^2}}\right), \tag{B1}$$

$$\frac{\partial\overline{\theta_l'^3}}{\partial\beta} = \frac{1}{(1-\tilde{\sigma}_w^2)^2}\frac{\overline{w'^3}}{(\overline{w'^2})^2}\overline{\theta_l'^2}\,\overline{w'\theta_l'}\left(1 - \frac{1}{1-\tilde{\sigma}_w^2}\frac{(\overline{w'\theta_l'})^2}{\overline{w'^2}\,\overline{\theta_l'^2}}\right), \tag{B2}$$

$$\frac{\partial\overline{w'^4}}{\partial\gamma} = [1 - \max(c_{w\theta_l}^2, c_{wq_t}^2)]\left[4(1-\tilde{\sigma}_w^2)(\overline{w'^2})^2 + \frac{1}{(1-\tilde{\sigma}_w^2)^2}\frac{(\overline{w'^3})^2}{\overline{w'^2}}\right], \tag{B3}$$

$$\frac{\partial\overline{w'^4}}{\partial\beta} = 0, \tag{B4}$$

$$\frac{\partial\overline{w'^2\theta_l'}}{\partial\gamma} = [1 - \max(c_{w\theta_l}^2, c_{wq_t}^2)]\frac{1}{(1-\tilde{\sigma}_w^2)^2}\frac{\overline{w'^3}}{\overline{w'^2}}\overline{w'\theta_l'}, \tag{B5}$$

$$\frac{\partial\overline{w'^2\theta_l'}}{\partial\beta} = 0, \tag{B6}$$

$$\frac{\partial \overline{w'\theta_l'^2}}{\partial \gamma} = [1 - \max(c_{w\theta_l}^2, c_{wq_t}^2)] \frac{1}{(1 - \tilde{\sigma}_w^2)^2} \frac{\overline{w'^3}}{\overline{w'^2}} \left[\frac{1}{3} \beta \overline{\theta_l'^2} + 2 \frac{\left(1 - \frac{1}{3}\beta\right)}{(1 - \tilde{\sigma}_w^2)} \frac{(\overline{w'\theta_l'})^2}{\overline{w'^2}} \right], \tag{B7}$$

$$\frac{\partial \overline{w'\theta_l'^2}}{\partial \beta} = \frac{1}{(1 - \tilde{\sigma}_w^2)} \frac{\overline{w'^3}}{\overline{w'^2}} \left[\frac{1}{3} \overline{\theta_l'^2} - \frac{1}{3} \frac{1}{(1 - \tilde{\sigma}_w^2)} \frac{(\overline{w'\theta_l'})^2}{\overline{w'^2}} \right], \tag{B8}$$

$$\frac{\partial \overline{w'q_t'\theta_l'}}{\partial \gamma} = \frac{[1 - \max(c_{w\theta_l}^2, c_{wq_t}^2)]}{(1 - \tilde{\sigma}_w^2)^2} \frac{\overline{w'^3}}{\overline{w'^2}} \left[\frac{1}{3} \beta \overline{q_t'\theta_l'} + 2 \frac{1 - \frac{1}{3}\beta}{(1 - \tilde{\sigma}_w^2)} \frac{\overline{w'q_t'}\,\overline{w'\theta_l'}}{\overline{w'^2}} \right], \tag{B9}$$

$$\frac{\partial \overline{w'q_t'\theta_l'}}{\partial \beta} = \frac{1}{(1 - \tilde{\sigma}_w^2)} \frac{\overline{w'^3}}{\overline{w'^2}} \left[\frac{1}{3} \overline{q_t'\theta_l'} - \frac{1}{3} \frac{1}{(1 - \tilde{\sigma}_w^2)} \frac{\overline{w'q_t'}\,\overline{w'\theta_l'}}{\overline{w'^2}} \right]. \tag{B10}$$

We note a few features of these sensitivities:

1) For all higher-order moments except $\overline{w'^4}$, the sensitivity with respect to changes in γ depends on some power of $1/(1 - \tilde{\sigma}_w^2)$. This factor becomes large as $\gamma \to 1$ while $\max(c_{w\theta_l}^2, c_{wq_t}^2) < 1$. Therefore, as γ increases in magnitude, the sensitivity to changes in γ also increases. For the same reason, when γ is large, $\overline{\theta_l'^3}$, $\overline{w'\theta_l'^2}$, and $\overline{w'q_t'\theta_l'}$ are also sensitive to changes in β.
2) Because β appears linearly in the moment equations, the sensitivity with respect to changes in β does not depend on the value of β itself, but only on the known moments and γ.
3) For all moments, the sensitivity to changes in γ is proportional to $[1 - \max(c_{w\theta_l}^2, c_{wq_t}^2)]$. Consequently, the sensitivity to γ decreases as $\max(c_{w\theta_l}^2, c_{wq_t}^2) \to 1$.
4) For all higher-order moments except $\overline{w'^4}$, the sensitivity on γ and β depends linearly on $\overline{w'^3}$. Therefore, as $\overline{w'^3}$ or Sk_w approaches zero, the sensitivities tend to become small.

REFERENCES

Abdella, K., and N. McFarlane, 1997: A new second-order turbulence closure scheme for the planetary boundary layer. *J. Atmos. Sci.,* **54,** 1850–1867.

——, and A. C. Petersen, 2000: Third-order moment closure through a mass-flux approach. *Bound.-Layer Meteor.,* **95,** 303–318.

André, J. C., G. de Moor, P. Lacarrère, and R. du Vachat, 1978: Modeling the 24-hour evolution of the mean and turbulent structures of the planetary boundary layer. *J. Atmos. Sci.,* **35,** 1861–1883.

Bony, S., and K. A. Emanuel, 2001: A parameterization of the cloudiness associated with cumulus convection; evaluation using TOGA COARE data. *J. Atmos. Sci.,* **58,** 3158–3183.

Canuto, V. M., Y. Cheng, and A. Howard, 2001: New third-order moments for the convective boundary layer. *J. Atmos. Sci.,* **58,** 1169–1172.

Chung, T. J., 2002: *Computational Fluid Dynamics.* Cambridge University Press, 1012 pp.

Clarke, R. H., A. J. Dyer, R. R. Brook, D. G. Reid, and A. J. Troup, 1971: The Wangara experiment: Boundary layer data. Tech. Paper 19, Division of Meteorological Physics, CSIRO, Australia, 341 pp.

Cotton, W. R., and Coauthors, 2003: RAMS 2001: Current status and future directions. *Meteor. Atmos. Phys.,* **82,** 5–29.

de Roode, S. R., P. G. Duynkerke, and A. P. Siebesma, 2000: Analogies between mass-flux and Reynolds-averaged equations. *J. Atmos. Sci.,* **57,** 1585–1598.

Deardorff, J. W., 1974: Three-dimensional numerical study of the height and mean structure of a heated planetary boundary layer. *Bound.-Layer Meteor.,* **7,** 81–106.

Golaz, J.-C., V. E. Larson, and W. R. Cotton, 2002a: A PDF-based model for boundary layer clouds. Part I: Method and model description. *J. Atmos. Sci.,* **59,** 3540–3551.

——, ——, and ——, 2002b: A PDF-based model for boundary layer clouds. Part II: Model results. *J. Atmos. Sci.,* **59,** 3552–3571.

Gryanik, V. M., and J. Hartmann, 2002: A turbulence closure for the convective boundary layer based on a two-scale mass-flux approach. *J. Atmos. Sci.,* **59,** 2729–2744.

Lappen, C.-L., and D. A. Randall, 2001: Toward a unified parameterization of the boundary layer and moist convection. Part I: A new type of mass-flux model. *J. Atmos. Sci.,* **58,** 2021–2036.

Larson, V. E., R. Wood, P. R. Field, J.-C. Golaz, T. H. Vonder Haar, and W. R. Cotton, 2001: Small-scale and mesoscale variability of scalars in cloudy boundary layers: One-dimensional probability density functions. *J. Atmos. Sci.,* **58,** 1978–1994.

——, J.-C. Golaz, and W. R. Cotton, 2002: Small-scale and mesoscale variability in cloudy boundary layers: Joint probability density functions. *J. Atmos. Sci.,* **59,** 3519–3539.

Lewellen, W. S., and S. Yoh, 1993: Binormal model of ensemble partial cloudiness. *J. Atmos. Sci.,* **50,** 1228–1237.

Mellor, G. L., 1977: The Gaussian cloud model relations. *J. Atmos. Sci.,* **34,** 356–358.

Mironov, D. V., V. M. Gryanik, V. N. Lykossov, and S. S. Zilitinkevich, 1999: Comments on "A new second-order turbulence closure scheme for the planetary boundary layer." *J. Atmos. Sci.,* **56,** 3478–3481.

Moeng, C.-H., and Coauthors, 1996: Simulation of a stratocumulus-topped planetary boundary layer: Intercomparison among different numerical codes. *Bull. Amer. Meteor. Soc.,* **77,** 261–278.

Pope, S. B., 2000: *Turbulent Flows.* Cambridge University Press, 771 pp.

Randall, D. A., Q. Shao, and C.-H. Moeng, 1992: A second-order bulk boundary-layer model. *J. Atmos. Sci.,* **49,** 1903–1923.

Siebesma, A. P., and Coauthors, 2003: A large eddy simulation intercomparison study of shallow cumulus convection. *J. Atmos. Sci.,* **60,** 1201–1219.

Smith, R. N. B., 1990: A scheme for predicting layer clouds and their water content in a general circulation model. *Quart. J. Roy. Meteor. Soc.,* **116,** 435–460.

Sommeria, G., and J. W. Deardorff, 1977: Subgrid-scale condensation in models of nonprecipitating clouds. *J. Atmos. Sci.,* **34,** 344–355.

Tompkins, A. M., 2002: A prognostic parameterization for the subgrid-scale variability of water vapor and clouds in large-scale models and its use to diagnose cloud cover. *J. Atmos. Sci.,* **59,** 1917–1942.

Wang, S., and B. Stevens, 2000: Top-hat representation of turbulence statistics in cloud-topped boundary layers: A large eddy simulation study. *J. Atmos. Sci.,* **57,** 423–441.

Zilitinkevich, S. S., V. M. Gryanik, V. N. Lykossov, and D. V. Mironov, 1999: Third-order transport and nonlocal turbulence closures for convective boundary layers. *J. Atmos. Sci.,* **56,** 3463–3477.